and stopped by adding 5 μL helicase termination buffer consisting of 0.1 M Tris-HCl (pH 7.5), 20 mM EDTA, 0.5% SDS, 0.1% Nonidet P-40, 0.1% bromophenol blue, 0.1% xylene cyanol, and 25% glycerol. The terminated reaction mixture was subjected to native TBE 10% polyacrylamide gel electrophoresis. The radioactive RNAs in the gel were visualized with an Image Reader FLA-9000 (Fujifilm) and quantified by Multi Gauge V 3.11 software.

3.5. RNA Binding Assay

RNA binding to NS3 helicase was analyzed by gel mobility shift assay [40]. First, let-7 single-strand RNA (5'-UGAGGUAGUAGGUUGUAUAGU-3') was incubated with [γ-^{32}P] ATP (Muromachi, Tokyo, Japan) and T4 polynucleotide kinase (Toyobo) at 37 °C for 60 min for labeling at the 5'-end of the single-strand RNA. The reaction mixture was subjected to phenol chloroform extraction for purification of labeled RNA. The reaction was carried out at room temperature for 15 min in 20 μL of the mixture consisting of 30 mM Tris-HCl (pH 7.5), 100 mM NaCl, 2 mM $MgCl_2$, 1 mM DTT, 1 unit of RNasin Plus (Promega) per microliter, 300 nM NS3, 5 fmol let-7-labeled ssRNA, and an indicated concentration of SG1-23-1. The reaction was stopped by adding an equal volume of dye solution consisting of 0.025% bromophenol blue, 10% glycerol, and 0.5× Tris/borate/EDTA (TBE). The resulting mixture was subjected to native 6% polyacrylamide gel electrophoresis (acrylamide: bis acrylamide = 19:1). The radioactive RNA was visualized with the Image Reader FLA-9000 and quantified by Multi Gauge V 3.11 software.

3.6. Cell Lines

The following Huh-7-derived cell lines used in this study were maintained in Dulbecco's modified Eagle's medium containing 10% fetal calf serum and 0.5 mg/mL G418: The Lunet/Con1 LUN Sb #26 cell line, which harbors the subgenomic replicon RNA of the Con1 strain (genotype 1b) [34]; the Huh7/ORN3-5B #24 cell line, which harbors the subgenomic replicon RNA of the O strain (genotype 1b) [35]; the Huh7 Rep Feo cell line, which harbors the subgenomic replicon RNA of the N strain (genotype 1b) [33]; and the OR6 cell line, which harbors the full genomic RNA of the O strain (genotype 1b) [35].

3.7. Determination of Luciferase Activity in HCV Replicon Cells

HCV replicon cells were seeded at 2×10^4 cells per well in a 48-well plate 24 h before treatment. The extract SG1-23-1 was added to the culture medium at various concentrations. The treated cells were harvested 72 h post-treatment and lysed in cell culture lysis reagent (Promega) or *Renilla* luciferase assay lysis buffer (Promega). Luciferase activity in the harvested cells was estimated with a luciferase assay system (Promega) or a *Renilla* luciferase assay system (Promega). The resulting luminescence was detected by the Luminescencer-JNR AB-2100 (ATTO, Tokyo, Japan) and corresponded to the expression level of the HCV replicon.

3.8. Determination of Cytotoxicity in HCV Replicon Cells

HCV replicon cells were seeded at a density of 1×10^4 cells per well in a 96-well plate and incubated at 37 °C for 24 h. The extract fraction of the sample code SG1-23-1 was added to the culture medium at various concentrations. These cells were treated with an indicated concentration of the extract fraction and then were harvested 72 h post-treatment. Cell viability was measured by dimethylthiazol carboxymethoxy-phenylsulfophenyl tetrazolium (MTS) assay using a CellTiter 96 aqueous one-solution cell proliferation assay kit (Promega).

3.9. Effects on Activities of Luciferase and Internal Ribosome Entry Site (IRES)

The plasmid pEF Fluc IN and pEF Rluc EMCV IRES Feo were described previously [41]. The firefly luciferase gene was replaced with the *Renilla* luciferase gene in the plasmid pEF Fluc IN. The resulting plasmid was designated as pEF RlucIN in this study. The Huh7 cells were transfected with the pEF Fluc IN, pEF Rluc IN, or pEF Rluc EMCV IRES Feo and then were established in a medium containing 0.25 mg/mL G418 as described previously [41]. These cell lines were seeded at 2×10^4 cells per well in a 48-well plate 24 h before treatment, treated with 50 μg/mL extract SG1-23-1, and then harvested at 72 h post-treatment. Activities of firefly and *Renilla* luciferases in pEF Rluc EMCV IRES Feo were measured with the dual luciferase reporter assay system (Promega). Total protein concentration was measured using the BCA Protein Assay Reagent Kit (Thermo Scientific, Rockford, IL, USA) to normalize luciferase activity.

3.10. Western Blotting

The cells were lysed in lysis buffer containing Cell Culture Lysis Reagent (Promega). The cell lysate was subjected to SDS-10% polyacrylamide gel (SDS-PAGE). The proteins in the gel were transferred onto a polyvinylidene fluoride (PVDF) membrane. The resulting membrane was incubated with the primary antibodies at 4 °C overnight and then was washed three times with PBS containing 0.02% Tween 20 (PBS-T). The resulting membrane was reacted with a horseradish peroxidase-labeled anti-IgG antibody at room temperature for 2 h and then was washed three times with PBS-T. The reacted proteins were visualized with ImmunoStar LD (Wako Pure Chemical, Osaka, Japan). The antibodies to NS3 (Abcam, Cambridge, UK), NS5A (ViroGen, Watertown, MA, USA) and beta-actin were purchased from New England Biolabs (Beverly, MA, USA) and were used as the primary antibodies in this study.

3.11. Reverse-Transcription Polymerase Chain Reaction (RT-PCR)

The previously described method of RT-PCR [41] was slightly modified, as described below. Total RNA was isolated from cultured cells with the RNAqueous-4PCR kit (Ambion, Austin, TX, USA) and then was reverse-transcribed with a Superscript III reverse transcriptase (Invitrogen, Carlsbad, CA, USA). The transcribed mRNA was amplified with PCR using AmpliTaq Gold DNA polymerase (Applied Biosystems, Foster City, CA, USA) and an appropriate primer pair. Primer sequences targeting the genes encoding 2',5'-oligoadenylate synthetase (2',5'-OAS), myxovirus resistance protein A (MxA), and glyceraldehyde-3-phosphate dehydrogenase (GAPDH) were described previously [41].

4. Conclusions

In conclusion, we showed that the ethyl acetate extract from *Alloeocomatella polycladia* significantly inhibits HCV replication by suppressing viral helicase activity. The purification of an inhibitory compound from the extract of *Alloeocomatella polycladia* will be required in order to improve the efficacy of chemical modification of the compound(s).

Acknowledgments

We thank R. Bartenschlager for kindly providing cell lines and plasmids, and H. Kasai and I. Katoh for their helpful comments and discussions. This work was supported in part by grants-in-aid from the Ministry of Health, Labor (H22-kanen-004, 006 and 009), and Welfare and from the Ministry of Education, Culture, Sports, Science, and Technology of Japan.

References

1. Baldo, V.; Baldovin, T.; Trivello, R.; Floreani, A. Epidemiology of HCV infection. *Curr. Pharm. Des.* **2008**, *14*, 1646–1654.
2. Seeff, L.B. Natural history of chronic hepatitis C. *Hepatology* **2002**, *36*, S35–S46.
3. Moriishi, K.; Matsuura, Y. Host factors involved in the replication of hepatitis C virus. *Rev. Med. Virol.* **2007**, *17*, 343–354.
4. Tsukiyama-Kohara, K.; Iizuka, N.; Kohara, M.; Nomoto, A. Internal ribosome entry site within hepatitis C virus RNA. *J. Virol.***1992**, *66*, 1476–1483.
5. Bartenschlager, R.; Ahlborn-Laake, L.; Mous, J.; Jacobsen, H. Nonstructural protein 3 of the hepatitis C virus encodes a serine-type proteinase required for cleavage at the NS3/4 and NS4/5 junctions. *J. Virol.* **1993**, *67*, 3835–3844.
6. Kim, D.W.; Gwack, Y.; Han, J.H.; Choe, J. *C*-terminal domain of the hepatitis C virus NS3 protein contains an RNA helicase activity. *Biochem. Biophys. Res. Commun.* **1995**, *215*, 160–166.
7. Failla, C.; Tomei, L.; de Francesco, R. Both NS3 and NS4A are required for proteolytic processing of hepatitis C virus nonstructural proteins. *J. Virol.* **1994**, *68*, 3753–3760.
8. Belon, C.A.; Frick, D.N. Helicase inhibitors as specifically targeted antiviral therapy for hepatitis C. *Future Virol.* **2009**, *4*, 277–293.
9. Frick, D.N. The hepatitis C virus NS3 protein: a model RNA helicase and potential drug target. *Curr. Issues Mol. Biol.* **2007**, *9*, 1–20.
10. Kwong, A.D.; Rao, B.G.; Jeang, K.T. Viral and cellular RNA helicases as antiviral targets. *Nat. Rev. Drug Discov.* **2005**, *4*, 845–853.
11. Manns, M.P.; Wedemeyer, H.; Cornberg, M. Treating viral hepatitis C: efficacy, side effects, and complications. *Gut* **2006**, *55*, 1350–1359.
12. McHutchison, J.G.; Everson, G.T.; Gordon, S.C.; Jacobson, I.M.; Sulkowski, M.; Kauffman, R.; McNair, L.; Alam, J.; Muir, A.J.; Team, P.S. Telaprevir with peginterferon and ribavirin for chronic HCV genotype 1 infection. *N. Engl. J. Med.* **2009**, *360*, 1827–1838.

13. Zeuzem, S.; Hultcrantz, R.; Bourliere, M.; Goeser, T.; Marcellin, P.; Sanchez-Tapias, J.; Sarrazin, C.; Harvey, J.; Brass, C.; Albrecht, J. Peginterferon alfa-2b plus ribavirin for treatment of chronic hepatitis C in previously untreated patients infected with HCV genotypes 2 or 3. *J. Hepatol.* **2004**, *40*, 993–999.
14. Asselah, T.; Marcellin, P. New direct-acting antivirals' combination for the treatment of chronic hepatitis C. *Liver Int.* **2011**, *31 Suppl 1*, 68–77.
15. Jazwinski, A.B.; Muir, A.J. Direct-acting antiviral medications for chronic hepatitis C virus infection. *Gastroenterol. Hepatol. (NY)* **2011**, *7*, 154–162.
16. Lange, C.M.; Sarrazin, C.; Zeuzem, S. Review article: specifically targeted anti-viral therapy for hepatitis C—A new era in therapy. *Aliment. Pharmacol. Ther.* **2010**, *32*, 14–28.
17. Hofmann, W.P.; Zeuzem, S. A new standard of care for the treatment of chronic HCV infection. *Nat. Rev. Gastroenterol. Hepatol.* **2011**, *8*, 257–264.
18. Kwong, A.D.; Kauffman, R.S.; Hurter, P.; Mueller, P. Discovery and development of telaprevir: An NS3-4A protease inhibitor for treating genotype 1 chronic hepatitis C virus. *Nat. Biotechnol.* **2011**, *29*, 993–1003.
19. Kieffer, T.L.; Kwong, A.D.; Picchio, G.R. Viral resistance to specifically targeted antiviral therapies for hepatitis C (STAT-Cs). *J. Antimicrob. Chemother.* **2010**, *65*, 202–212.
20. Thompson, A.J.; McHutchison, J.G. Antiviral resistance and specifically targeted therapy for HCV (STAT-C). *J. Viral. Hepat.* **2009**, *16*, 377–387.
21. Belon, C.A.; High, Y.D.; Lin, T.I.; Pauwels, F.; Frick, D.N. Mechanism and specificity of a symmetrical benzimidazolephenylcarboxamide helicase inhibitor. *Biochemistry* **2010**, *49*, 1822–1832.
22. Maga, G.; Gemma, S.; Fattorusso, C.; Locatelli, G.A.; Butini, S.; Persico, M.; Kukreja, G.; Romano, M.P.; Chiasserini, L.; Savini, L.; *et al.* Specific targeting of hepatitis C virus NS3 RNA helicase. Discovery of the potent and selective competitive nucleotide-mimicking inhibitor QU663. *Biochemistry* **2005**, *44*, 9637–9644.
23. Chin, Y.W.; Balunas, M.J.; Chai, H.B.; Kinghorn, A.D. Drug discovery from natural sources. *AAPS J.* **2006**, *8*, E239–E253.
24. Koehn, F.E.; Carter, G.T. The evolving role of natural products in drug discovery. *Nat. Rev. Drug Discov.* **2005**, *4*, 206–220.
25. Li, J.W.; Vederas, J.C. Drug discovery and natural products: End of an era or an endless frontier? *Science* **2009**, *325*, 161–165.
26. Ahmed-Belkacem, A.; Ahnou, N.; Barbotte, L.; Wychowski, C.; Pallier, C.; Brillet, R.; Pohl, R.T.; Pawlotsky, J.M. Silibinin and related compounds are direct inhibitors of hepatitis C virus RNA-dependent RNA polymerase. *Gastroenterology* **2010**, *138*, 1112–1122.
27. Wagoner, J.; Negash, A.; Kane, O.J.; Martinez, L.E.; Nahmias, Y.; Bourne, N.; Owen, D.M.; Grove, J.; Brimacombe, C.; McKeating, J.A.; *et al.* Multiple effects of silymarin on the hepatitis C virus lifecycle. *Hepatology* **2010**, *51*, 1912–1921.
28. Ciesek, S.; von Hahn, T.; Colpitts, C.C.; Schang, L.M.; Friesland, M.; Steinmann, J.; Manns, M.P.; Ott, M.; Wedemeyer, H.; Meuleman, P.; *et al.* The green tea polyphenol, epigallocatechin-3-gallate, inhibits hepatitis C virus entry. *Hepatology* **2011**, *54*, 1947–1955.

29. Takeshita, M.; Ishida, Y.; Akamatsu, E.; Ohmori, Y.; Sudoh, M.; Uto, H.; Tsubouchi, H.; Kataoka, H. Proanthocyanidin from blueberry leaves suppresses expression of subgenomic hepatitis C virus RNA. *J. Biol. Chem.* **2009**, *284*, 21165–21176.
30. Donia, M.; Hamann, M.T. Marine natural products and their potential applications as anti-infective agents. *Lancet Infect. Dis.* **2003**, *3*, 338–348.
31. Molinski, T.F.; Dalisay, D.S.; Lievens, S.L.; Saludes, J.P. Drug development from marine natural products. *Nat. Rev. Drug Discov.* **2009**, *8*, 69–85.
32. Mayer, A.M.; Glaser, K.B.; Cuevas, C.; Jacobs, R.S.; Kem, W.; Little, R.D.; McIntosh, J.M.; Newman, D.J.; Potts, B.C.; Shuster, D.E. The odyssey of marine pharmaceuticals: A current pipeline perspective. *Trends Pharmacol. Sci.* **2010**, *31*, 255–265.
33. Yokota, T.; Sakamoto, N.; Enomoto, N.; Tanabe, Y.; Miyagishi, M.; Maekawa, S.; Yi, L.; Kurosaki, M.; Taira, K.; Watanabe, M.; *et al.* Inhibition of intracellular hepatitis C virus replication by synthetic and vector-derived small interfering RNAs. *EMBO Rep.* **2003**, *4*, 602–608.
34. Frese, M.; Barth, K.; Kaul, A.; Lohmann, V.; Schwarzle, V.; Bartenschlager, R. Hepatitis C virus RNA replication is resistant to tumour necrosis factor-alpha. *J. Virol.* **2003**, *84*, 1253–1259.
35. Ikeda, M.; Abe, K.; Dansako, H.; Nakamura, T.; Naka, K.; Kato, N. Efficient replication of a full-length hepatitis C virus genome, strain O, in cell culture, and development of a luciferase reporter system. *Biochem. Biophys. Res. Commun.* **2005**, *329*, 1350–1359.
36. Blight, K.J.; Kolykhalov, A.A.; Rice, C.M. Efficient initiation of HCV RNA replication in cell culture. *Science* **2000**, *290*, 1972–1974.
37. Guo, J.T.; Bichko, V.V.; Seeger, C. Effect of alpha interferon on the hepatitis C virus replicon. *J. Virol.***2001**, *75*, 8516–8523.
38. Tani, H.; Akimitsu, N.; Fujita, O.; Matsuda, Y.; Miyata, R.; Tsuneda, S.; Igarashi, M.; Sekiguchi, Y.; Noda, N. High-throughput screening assay of hepatitis C virus helicase inhibitors using fluorescence-quenching phenomenon. *Biochem. Biophys. Res. Commun.* **2009**, *379*, 1054–1059.
39. Gallinari, P.; Brennan, D.; Nardi, C.; Brunetti, M.; Tomei, L.; Steinkuhler, C.; De Francesco, R. Multiple enzymatic activities associated with recombinant NS3 protein of hepatitis C virus. *J. Virol.* **1998**, *72*, 6758–6769.
40. Huang, Y.; Liu, Z.R. The ATPase, RNA unwinding, and RNA binding activities of recombinant p68 RNA helicase. *J. Biol. Chem.* **2002**, *277*, 12810–12815.
41. Jin, H.; Yamashita, A.; Maekawa, S.; Yang, P.; He, L.; Takayanagi, S.; Wakita, T.; Sakamoto, N.; Enomoto, N.; Ito, M. Griseofulvin, an oral antifungal agent, suppresses hepatitis C virus replication *in vitro*. *Hepatol. Res.* **2008**, *38*, 909–918.

AAC
Journals.ASM.org

Anti-Human Immunodeficiency Virus Type 1 Activity of Novel 6-Substituted 1-Benzyl-3-(3,5-Dimethylbenzyl)Uracil Derivatives

Paula Ordonez,[a] Takayuki Hamasaki,[a] Yohei Isono,[b] Norikazu Sakakibara,[b] Masahiro Ikejiri,[c] Tokumi Maruyama,[b] and Masanori Baba[a]

Division of Antiviral Chemotherapy, Center for Chronic Viral Diseases, Graduate School of Medical and Dental Sciences, Kagoshima University, Kagoshima, Japan[a]; Faculty of Pharmaceutical Sciences at Kagawa Campus, Tokushima Bunri University, Sanuki, Japan[b]; and Faculty of Pharmacy, Osaka Ohtani University, Tondabayashi, Japan[c]

Nonnucleoside reverse transcriptase (RT) inhibitors (NNRTIs) are important components of current combination therapies for human immunodeficiency virus type 1 (HIV-1) infection. In screening of chemical libraries, we found 6-azido-1-benzyl-3-(3,5-dimethylbenzyl)uracil (AzBBU) and 6-amino-1-benzyl-3-(3,5-dimethylbenzyl)uracil (AmBBU) to be highly active and selective inhibitors of HIV-1 replication *in vitro*. To determine the resistance profiles of these compounds, we conducted a long-term culture of HIV-1-infected MT-4 cells with escalating concentrations of each compound. After serial passages of the infected cells, escape viruses were obtained, and they were more than 500-fold resistant to the uracil derivatives compared to the wild type. Sequence analysis was conducted for RT of the escape viruses at passages 12 and 24. The amino acid mutation Y181C in the polymerase domain of RT was detected for all escape viruses. Docking studies using the crystal structure of RT showed that AmBBU requires the amino acid residues Leu100, Val106, Tyr181, and Trp229 for exerting its inhibitory effect on HIV-1. Four additional amino acid changes (K451R, R461K, T468P, and D471N) were identified in the RNase H domain of RT; however, their precise role in the acquisition of resistance is still unclear. In conclusion, the initial mutation Y181C seems sufficient for the acquisition of resistance to the uracil derivatives AzBBU and AmBBU. Further studies are required to determine the precise role of each mutation in the acquisition of HIV-1 resistance.

Human immunodeficiency virus type 1 (HIV-1) reverse transcriptase (RT) is responsible for synthesizing a double-stranded integrative cDNA from the single-stranded viral genomic RNA in the early virus life cycle. HIV-1 RT is a heterodimer composed of two subunits, p66 and p51, and p51 is generated by the proteolytic processing and removal of C terminus (amino acids 441 to 560) from p66 (32). The p66 subunit is composed of two spatially distinct domains: polymerase (residues 1 to 426) and RNase H (residues 427 to 560). The polymerase domain is composed of four subdomains: fingers (residues 1 to 85 and 118 to 155), palm (residues 86 to 117 and 156 to 236), thumb (237 to 318), and connection (319 to 426) (46). The polymerase domain creates a copy of the viral genome, while the RNase H domain promotes RNA degradation from the DNA/RNA duplex during reverse transcription. Other RNase H functions include the removal of $tRNA_3^{Lys}$, and the polypurine tract, which are primers for minus- and plus-strand DNA synthesis (11, 47, 58).

The polymerase domain is currently targeted by two classes of antiretroviral drugs, nucleoside RT inhibitors (NRTIs) and nonnucleoside RT inhibitors (NNRTIs). NNRTIs are important components of current antiretroviral therapies for HIV-1. To date, more than 50 structurally diverse classes of compounds have been identified as genuine NNRTIs (60). Earlier NNRTIs include nevirapine (NVP), delavirdine (DLV), and efavirenz (EFV), and recent NNRTIs include etravirine (ETR). Several other NNRTIs, such as emivirine (MKC-442), underwent clinical trials, and yet they were not approved due to unfavorable pharmacokinetics, insufficient efficacy, and/or safety concerns (50). Recently, rilpivirine (RPV; formerly TMC278) has been formally licensed for clinical use in treatment-naive adult patients (56), while other NNRTIs, including IDX899, RDEA-428, and lersivirine, are currently under clinical development (1, 12, 30).

Although NNRTIs are generally well tolerated, a major limitation for all currently available NNRTIs is the low genetic barrier to resistance, which allows rapid emergence of drug resistance caused by a small number of amino acid mutations in the target region. HIV-1 drug resistance mutations in RT are extensively characterized for NRTIs and NNRTIs (29). NNRTIs inhibit HIV-1 by allosteric binding to a hydrophobic pocket in the RT about 10 Å behind the catalytic site (48). The positions associated with NNRTI resistance that make up the central NNRTI binding pocket are L100, K101, K103, V106, V108, V179, Y181, Y188, G190, F227, and W229. Additional positions that make up the pocket include E138, which is contributed by the p51 subunit, and M230, L234, P236, K238, and Y318, which form part of an extended pocket. Additional accessory NNRTI resistance abutting positions that form the NNRTI binding pocket include A98 and P225.

Mutations that are selected after failure of treatment with NNRTIs are located in the enzyme hydrophobic pocket, and they reduce the binding affinity of the inhibitors to the enzyme (7). A single mutation in the NNRTI-binding pocket may confer high-level resistance to one or more NNRTIs. Since NVP, DLV, and EFV have similar binding modes to RT, viruses resistant to one of these compounds develop cross-resistance to the others. ETR maintains its activity against NVP-, DLV-, or EFV-resistant mutants due to its ability of multiple binding modes to RT.

In order to improve the design of novel NNRTIs for future clinical development, *in vitro* isolation and analyses of drug-resis-

Received 8 December 2011 **Returned for modification** 5 January 2012
Accepted 24 January 2012
Published ahead of print 30 January 2012
Address correspondence to Masanori Baba, m-baba@m2.kufm.kagoshima-u.ac.jp.

doi:10.1128/AAC.06307-11

tant viruses are necessary to obtain valuable information on the resistance patterns of novel compounds. We previously synthesized and evaluated nine novel uracil analogues as NNRTIs, including four 1-substituted 3-(3,5-dimethylbenzyl)-5-fluorouracils and five 6-substituted 1-benzyl-3-(3,5-dimethylbenzyl)uracils (28). Two of these compounds—6-azido-1-benzyl-3-(3,5-dimethylbenzyl)uracil (AzBBU) and 6-amino-1-benzyl-3-(3,5-dimethylbenzyl) uracil (AmBBU)—were found to be highly active and selective inhibitors of HIV-1 replication *in vitro*.

In the present study, we conducted a long-term culture experiment with HIV-1-infected MT-4 cells with escalating concentrations of AzBBU and AmBBU. After serial passages of the infected cells, escape viruses were obtained, which displayed complete resistance to these compounds. Sequence analysis of RT from escape viruses was performed to determine the mutations related to the acquisition of resistance.

MATERIALS AND METHODS

Compounds. AzBBU and AmBBU were synthesized as previously described (28). The lead compound 1-benzyl-3-(3,5-dimethylbenzyl) uracil (BBF-29), 6-benzyl-1-ethoxymethyl-5-isopropyluracil (MKC-442), and the nucleoside analog 2′,3′-didehydro-3′-deoxy-4′-ethynylthymidine (4′-Ed4T) were prepared according as previously described (25, 34, 52). All compounds were dissolved in dimethyl sulfoxide at 100 mM and stored at −20°C until use. The chemical structures of AzBBU, AmBBU, BBF-29, MKC-442, and 4′-Ed4T are shown in Fig. 1.

Cells and viruses. MT-4 and M8166 cells were maintained in RPMI 1640 medium supplemented with 10% heat-inactivated fetal bovine serum, 100 U of penicillin G/ml, and 100 μg of streptomycin/ml. The HIV-1 strain III_B, the HIV-1 resistance strain III_{B-R}, and the HIV-2 strain ROD were used throughout the antiviral experiments (Table 1). III_{B-R} is a NNRTI-resistant mutant established by a serial passage of infected cells in the presence of increasing concentrations of MKC-442 (5). Viruses were propagated and titrated in MT-4 cells (HIV-1) or M8166 cells (HIV-2). Virus stocks were stored at −80°C until use. Escape viruses obtained after long-term culture with AzBBU and AmBBU were used for the following anti-HIV-1 experiments (Table 2).

Antiviral assays. The antiviral activity of test compounds against HIV-1 and HIV-2 was determined by the inhibition of virus-induced cytopathic effect (CPE) (4). Briefly, MT-4 or M8166 cells (10^5 cells/ml) were infected with HIV-1 or HIV-2, respectively, at a multiplicity of infection (MOI) of 0.1 and were cultured in the presence of various concentrations of the tested compounds. After a 4-day incubation at 37°C, the number of viable cells was monitored by the 3-(4,5-dimethylthiazol-2-yl)-2,5-diphenyl-2*H*-tetrazolium bromide (MTT) method (39). The cytotoxicity of the compounds was evaluated in parallel with their antiviral activity, based on the viability of mock-infected cells, as determined by the MTT method. All experiments were performed in triplicate.

Long-term culture of infected MT-4 cells. MT-4 cells were infected with the HIV-1 strain III_B and incubated at 37°C for 4 days in the presence of compounds. The initial concentration of AzBBU and AmBBU corresponded to 2-fold higher than their 50% effective concentrations (EC_{50}s), i.e., 0.175 and 0.119 μM, respectively. As control cultures, exactly identical passages of the infected MT-4 cells in the absence of the compounds were carried out in parallel with the cultures exposed to the compounds. At each passage, virus-induced CPE of the cells was monitored to confirm virus replication. The concentration of each compound was escalated 2-fold, when the CPE in the compound-treated culture exceeded 70%. The escape viruses as well as the control viruses were propagated once in MT-4 cells, and they were used for further experiments.

Sequence analysis of RT. Genomic DNA was extracted from the infected MT-4 cells with a DNA extraction kit (Wako, Tokyo, Japan). The extracted DNA was quantified using a NanoDrop spectrophotometer ND-1000 (NanoDrop Technologies, Wilmington, DE) and subjected to nested PCR. Two regions of RT were amplified (RT1 and RT2). The first PCR consisted of an initial denaturation at 95°C for 2 min, followed by 40 cycles (95°C for 1 min, 46°C for 1 min, and 72°C for 1 min) and a final extension at 72°C for 5 min. The primers rt-1-f (5′-AGGGGGAATTGG AGGTTT-3′) and rt-1-r (5′-TCCCACAACTTCTGTATGTC-3′) were used to amplify the region RT1, and the primers rt-2-f (5′-ATGAACTCC ATCCTGATAAATG-3′) and rt-2-r (5′-TGTACAATCTAGTTGCCATA T-3′) were used to amplify the region RT2. The second PCR consisted of an initial denaturation at 95°C for 2 min, followed by 40 cycles (95°C for 1 min, 48°C for 1 min, and 72°C for 1 min) and a final extension at 72°C for 5 min. The primers rt-12-f (5′-CCAGTAAAATTAAAGCCAG-3′) and rt-12-r (5′-TCCCACTAACTTCTGTATGTC-3′) were used to amplify the region RT1, and the primers rt-22-f (5′-CCAGAAAAAGACAGCTG GACT-3′) and rt-22-r (5′-TGGCAGGTTAAAATCACTAGCC-3′) were used to amplify the region RT2. The second PCR generated fragments encompassing nucleotides 2120 to 2881 (RT1) and nucleotides 2834 to 3862 (RT2) of the RT gene corresponding to the HIV-1 complete genome (GenBank accession number AF033819). The amplified products were confirmed by capillary gel electrophoresis using the Agilent Bioanalyzer 2100 (Agilent Technologies, Palo Alto, CA). The PCR products were sequenced directly with a cycle sequence kit BigDye Terminator version 3.1 (Applied Biosystems, Foster City, CA), using both forward and reverse primers on an automated DNA analyzer model 3730 (Applied Biosystems), according to the manufacturer's instructions.

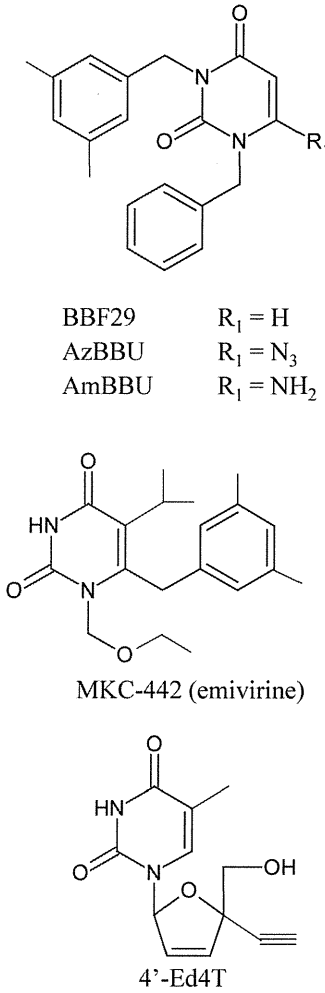

FIG 1 Structures of BBF-29, AzBBU, AmBBU, MKC-442, and 4′-Ed4T.

Docking study of compounds against HIV-1 RT. All *in silico* studies were performed using Molecular Operating Environment (MOE) soft-

TABLE 1 Antiviral activity of AzBBU and AmBBU against HIV-1 and HIV-2

Compound	Antiviral activity (mean EC_{50} [μM] and CC_{50} [μM] ± SD)[a] against:					
	HIV-1 III_B		HIV-1 III_{B-R}		HIV-2 ROD	
	EC_{50}	CC_{50}	EC_{50}	CC_{50}	EC_{50}	CC_{50}
AzBBU	0.088 ± 0.009	40.5 ± 6.7	>45.1	45.1 ± 0.5	>40.0	40.0 ± 2.7
AmBBU	0.060 ± 0.011	50.1 ± 1.1	>50.5	50.5 ± 6.3	>45.9	45.9 ± 1.2
BBF-29	0.26 ± 0.02	43.2 ± 9.1	13.9 ± 6.0	>100	>100	>100
MKC-442	0.015 ± 0.002	>100	6.2 ± 1.4	>100		
NVP	0.057 ± 0.005	>100	52.1 ± 23.6	>100		
4′-Ed4T	0.029 ± 0.008	>100	0.053 ± 0.038	>100	0.019 ± 0.007	>100

[a] EC_{50}, 50% effective concentration that inhibits virus-induced CPE of infected cells by 50%; CC_{50}, 50% cytotoxic concentration that reduces the viability of uninfected cells by 50%.The data represent the means for three independent experiments.

ware (Chemical Computing Group, Montreal, Quebec, Canada). The X-ray crystal structure of HIV-1 RT (PDB code 3m8p) (40) was downloaded from PDB at the Research Collaboration for Structural Bioinfomatics (http://www.rcsb.org/pdb/home/home.do) and optimized for the docking study by removing ligand and water, adding hydrogen atoms, assigning atomic charges, and minimizing using the Merck molecular force field 94X (MMFF94x) (22, 23, 55). Based on this structure, the structure of the HIV-1 RT (Y181C) was constructed. The docking site at the HIV-1 RT structure was searched by Alpha Site Finder, a function of MOE. Partial charges were added to the compound and a maximum of 250 conformers were generated using MMFF94x. MOE-ASEDock 2005 (Ryoka Systems, Tokyo, Japan) was then used for the docking of the compound to HIV-1 RT, and docking scores were calculated (19).

Statistical analysis. Statistical analysis for the EC_{50}s of the test compounds against the wild-type and resistant viruses was performed using an unpaired two-tailed Student *t* test. *P* values of <0.01 were considered statistically significant.

RESULTS

Antiviral activity of AzBBU and AmBBU against HIV-1 and HIV-2. AzBBU and AmBBU were tested for their inhibitory effects on the replication of HIV-1 III_B, HIV-1 III_{B-R}, and HIV-2 ROD. The NNRTIs BBF-29, MKC-442, and NVP, as well as the nucleoside analog 4′-Ed4T, were also tested for comparison. Their activities are given in Table 1. AzBBU and AmBBU showed high activity against HIV-1 III_B with similar EC_{50}s (0.088 ± 0.009 and 0.060 ± 0.011 μM, respectively) and 50% cytotoxic concentrations (CC_{50}s) (40.5 ± 6.7 and 50.1 ± 1.1 μM, respectively). AmBBU showed a higher selectivity index (SI) than AzBBU (SI = 835 versus SI = 460). These results are in accordance with those in the previous report (28). Although these compounds showed higher anti-HIV-1 activity against III_B compared to the lead compound BBF-29 (0.26 ± 0.02 μM), they were not active against the NNRTI-resistant HIV-1 stain III_{B-R}. In addition, AzBBU and AmBBU did not show any activity against HIV-2 ROD. In contrast, NRTI 4′-Ed4T was equally active against HIV-1 III_B, HIV-1 III_{B-R}, and HIV-2 ROD.

Isolation of escape viruses. Long-term cultures of HIV-1 (III_B strain)-infected MT-4 cells were started in the absence or presence of AzBBU and AmBBU (Fig. 2). The concentration of each compound was escalated 2-fold, when the CPE in the compound-treated culture exceeded 70%. At passage 24, the concentrations of AzBBU and AmBBU could reach 256-fold their EC_{50}s (22.4 and 15.2 μM, respectively). Viruses were isolated from culture supernatants at passages 12 and 24 (Fig. 2, points a, b, c, and d) and subjected to phenotypic and genotypic analyses.

Anti-HIV-1 activity of AzBBU and AmBBU against escape viruses. When AzBBU and AmBBU were examined for their activity against the escape viruses obtained at passages 12 and 24, the compounds did not show any significant inhibition at their nontoxic concentrations (Table 2). Thus, the isolates were more than 500-fold resistant to AzBBU and AmBBU compared to the wild type. The lead compound BBF-29 was also inactive against the escape viruses. The viruses had partial cross-resistance to MKC-442, probably due to its structural similarity (Fig. 1 and Table 2). NVP marginally inhibited the replication of the escape viruses. In contrast, 4′-Ed4T was equally inhibitory to the replication of the escape viruses and the wild type (Table 2).

TABLE 2 Anti-HIV-1 activity of AzBBU and AmBBU against escape viruses

Compound	Anti-HIV-1 activity (mean EC_{50} [μM] and CC_{50} [μM] ± SD)[a]							
	Passage 12				Passage 24			
	III_{B-AZ12}		III_{B-AM12}		III_{B-AZ24}		III_{B-AM24}	
	EC_{50}	CC_{50}	EC_{50}	CC_{50}	EC_{50}	CC_{50}	EC_{50}	CC_{50}
AzBBU	>44.5* (>500)	44.5 ± 0.3	>42.6* (>480)	42.6 ± 3.0	>43.6* (>500)	43.6 ± 0.5	>44.0* (>500)	44.0 ± 1.0
AmBBU	>60.7* (>1,000)	60.7 ± 6.5	>56.2* (>940)	56.2 ± 5.7	>48.1* (>800)	48.1 ± 4.8	>47.0* (>780)	47.0 ± 7.6
BBF-29	>46.4* (>180)	46.4 ± 9.5	>42.5* (>160)	42.5 ± 3.9	>49.4* (>190)	49.4 ± 3.0	>45.9* (>170)	45.9 ± 7.2
MKC-442	3.8 ± 1.2* (257)	>100	2.5 ± 0.6* (168)	>100	5.4 ± 3.5 (369)	>100	3.8 ± 1.2* (257)	>100
NVP	49.9 ± 10.9* (875)	>100	32.6 ± 4.6* (572)	>100	37.2 ± 3.5* (652)	>100	33.6 ± 6.7* (589)	>100
4′-Ed4T	0.038 ± 0.029 (1.3)	>100	0.092 ± 0.011* (3.2)	>100	0.028 ± 0.012 (1)	>100	0.023 ± 0.003 (0.8)	>100

[a] EC_{50}, 50% effective concentration that inhibits virus-induced CPE of infected cells by 50%; CC_{50}, 50% cytotoxic concentration that reduces the viability of uninfected cells by 50%. Fold changes, based on the EC_{50} for the wild type, are indicated in parentheses. The data represent the means for three independent experiments. Statistical analysis (Student *t* test) was performed for each EC_{50} compared to that of the wild type (*, $P < 0.01$).

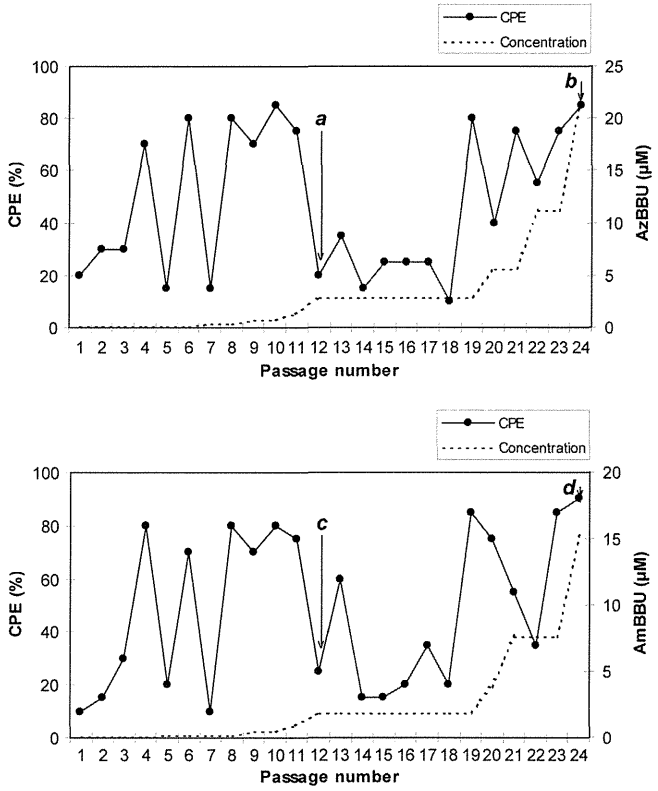

FIG 2 Long-term culture of infected MT-4 cells with escalating concentrations of AzBBU and AmBBU. MT-4 cells were infected with HIV-1 (III_B strain) and passaged every 4 days. Viral replication was monitored by determining the CPE of the cells at each passage. Culture supernatants from passages 12 and 24 were used for further experiments (CPE > 70%). Isolated viruses (points a, b, c, and d) were subjected to phenotypic and genotypic analyses. Points: a, passage 12, AzBBU ($III_{B\text{-}AZ12}$); b, passage 24, AzBBU ($III_{B\text{-}AZ24}$); c, passage 12, AmBBU ($III_{B\text{-}AM12}$); d, passage 24, AmBBU ($III_{B\text{-}AM24}$).

Amino acid changes of escape viruses. To determine what amino acid changes are associated with resistance to AzBBU and AmBBU, sequence analysis of full-length RT genes from escape viruses ($III_{B\text{-}AZ12}$, $III_{B\text{-}AM12}$, $III_{B\text{-}AZ24}$, $III_{B\text{-}AM24}$), as well as the wild-type control without treatment (III_B), was further performed at passages 12 and 24. The sequences of the escape viruses, III_B-AzBBU and III_B-AmBBU, were deposited in a public database (GenBank accession numbers JQ070415 and JQ070416). In addition, the sequence of the resistant strain $III_{B\text{-}R}$ was also analyzed for comparison (GenBank accession number JQ070417). Figure 3 shows the RT (subunit p66) amino acid sequences of escape viruses. Several synonymous mutations were observed in the RT gene. Overall, 5 amino acid changes were observed. One was in the polymerase domain, and four were in the RNase H domain. The same amino acid changes were detected at passages 12 and 24 (Fig. 3). Mutation Y181C in the polymerase domain was identified in all escape viruses. The resistant strain $III_{B\text{-}R}$ displayed the mutation V108I in addition to Y181C. Four additional amino acid changes (K451R, R461K, T468P, and D471N) were detected in the RNase H domain of all escape viruses.

Docking studies of AmBBU. Docking of the metabolically relevant derivative AmBBU to the binding-pocket of HIV-1 RT was performed. Figure 4 shows the proposed interactions between HIV-1 RT and AmBBU for HIV-1 RT wild type (Fig. 4A) and the mutant Y181C (Fig. 4B). AmBBU interacted with the amino acid residues Leu100, Val106, Tyr181, and Trp229 of HIV-1 RT (wt) through arene-H interactions (arene-H) (Fig. 4A), such as the hydrogen in the side chain of Leu100 with the central benzene ring (2-pyrimidine) of AmBBU, the hydrogen in the side chain of Val106 with 1-benzyl of AmBBU, the phenyl ring in the side chain of Tyr181 with hydrogen (3-methyl) at 3-(3,5-dimethylbenzyl) of AmBBU, and the indol ring in the side chain of Trp229 with 4′-hydrogen of 3-(3,5-dimethylbenzyl) of AmBBU (D2 representation in Fig. 4A). The compound lost the interaction at position 181 when replaced by cysteine (Y181C) (Fig. 4B). According to these data, the docking score between HIV-1 RT (wt) and AmBBU (−13.5110 kcal/mol) was higher than that between HIV-1 RT (Y181C) and AmBBU (−11.1648 kcal/mol).

DISCUSSION

Initially, we evaluated the antiviral activities of AzBBU and AmBBU against the HIV-1 strains III_B and $III_{B\text{-}R}$ and the HIV-2 strain ROD. AzBBU and AmBBU were highly active against III_B, and the EC_{50}s were similar for both compounds (Table 1). This is explainable, since the 6-azido uracil derivative (AzBBU) may be reduced metabolically to its 6-amino congener (AmBBU) in cell cultures (28). These compounds showed higher activity against III_B than the 1-substituted 3-(3,5-dimethylbenzyl)uracils previously reported (33). In contrast, AzBBU and AmBBU were not active against $III_{B\text{-}R}$, although the lead compound BBF-29 had weak activity. This may be due to the azido and amino groups introduced at 6-position of the 1-benzyl moiety, which is not present in BBF-29 (Fig. 1). Thus, 6-azido and 6-amino substitutions on the uracil ring increased the antiviral activity against III_B but decreased the antiviral activity against $III_{B\text{-}R}$. In addition, AzBBU and AmBBU did not show any activity against HIV-2 ROD. This is consistent with previous reports showing that HIV-2 is intrinsically resistant to most NNRTIs (14, 57). As expected, the nucleoside analog 4′-Ed4T was almost equally active against HIV-1 III_B, $III_{B\text{-}R}$, and HIV-2 ROD.

We isolated two HIV-1 strains highly resistant to AzBBU and AmBBU through long-term culture of HIV-1 III_B-infected MT-4 cells (Fig. 2). The phenotypic analysis revealed that escape viruses had partial cross-resistance to MKC-442, probably due to its structural similarity (Table 2 and Fig. 1). A similar finding has been reported for 1-[(2-hydroxyethoxy)methyl]-6-(phenylthio)thymine (HEPT) derivatives, where the HEPT-resistant virus also displayed cross-resistant to virtually all of other HIV-1-specific inhibitors, including NVP (6). 4′-Ed4T was equally active against the AzBBU- and AmBBU-resistant viruses compared to the wild type because of its different mechanism of action.

Our genotypic analysis revealed amino acid changes associated with resistance to AzBBU and AmBBU (Fig. 3). Several mutations were observed in the RT gene of resistant viruses, but some of them corresponded to synonymous mutations (Fig. 3). Amino acid changes were accumulated within a short period of cultivation (from passage 12, 48 days). Five amino acid changes were identified in all escape viruses at passages 12 and 24 (Fig. 3). They were attributable to the selection pressure by the compounds and were not the consequences of *in vitro* passage of infected cells, since these changes could be identified only for the escape viruses but not for the corresponding control viruses (data not shown).

We firstly identified the mutation Y181C within the polymerase domain of RT. Mutations responsible for NNRTI resistance

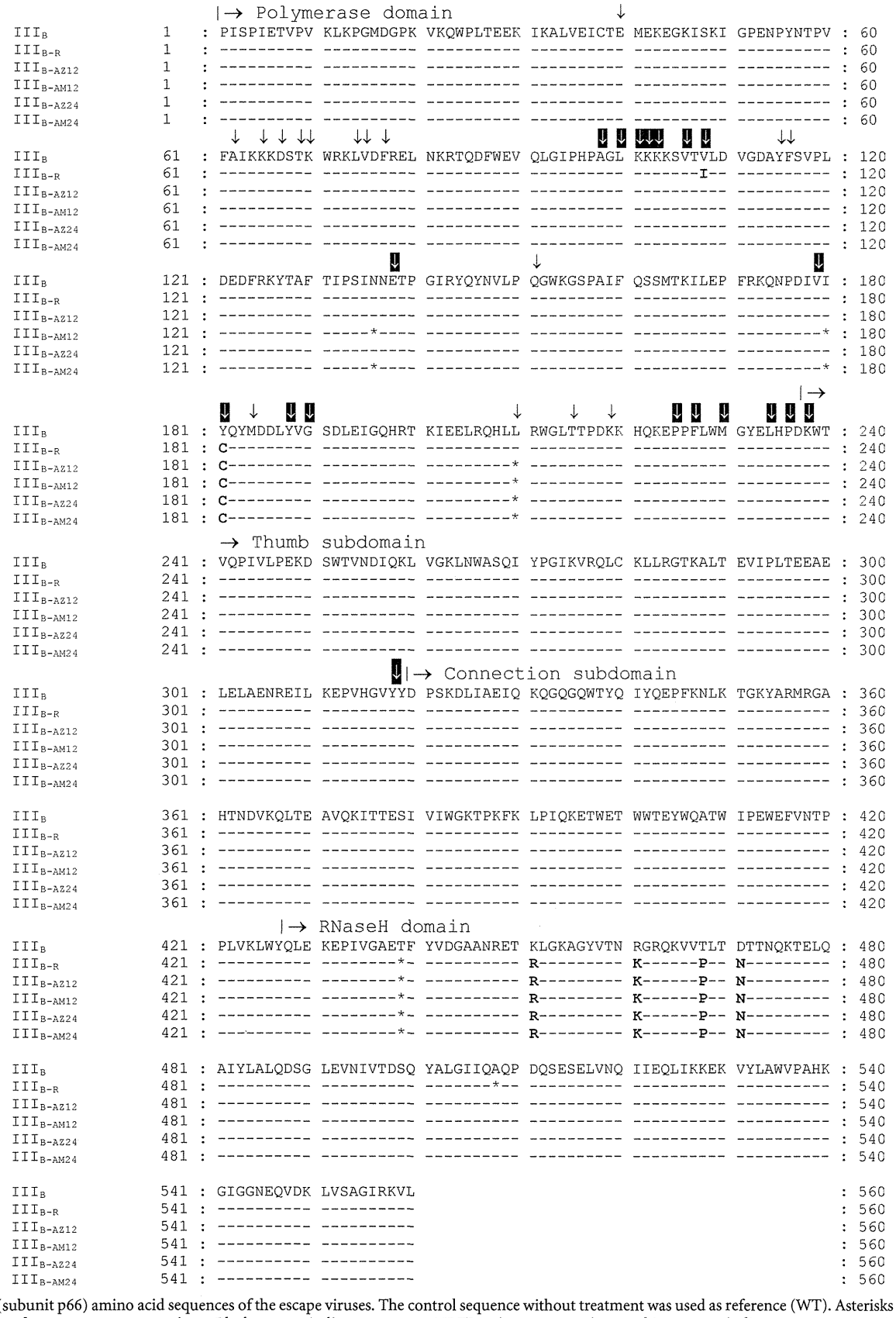

FIG 3 RT (subunit p66) amino acid sequences of the escape viruses. The control sequence without treatment was used as reference (WT). Asterisks (*) indicate the positions for synonymous mutations. Black arrows indicate common NRTI resistance mutations. White arrows indicate common NNRTI resistance mutations.

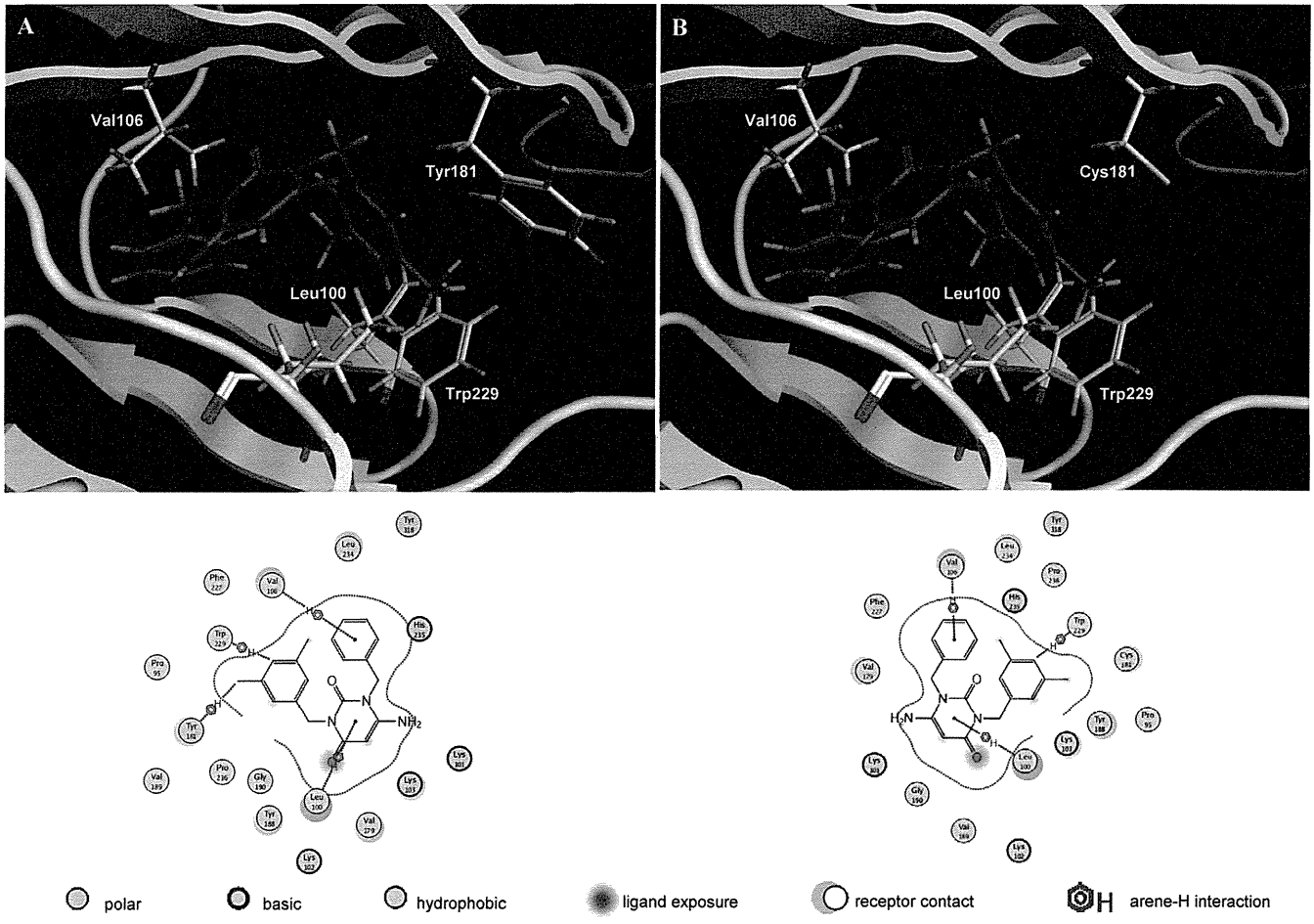

FIG 4 Docking of AmBBU to the binding pocket of HIV-1 RT. Docking structures between HIV-1 RT and AmBBU are shown for HIV-1 RT wt (A) and the mutant Y181C (B). The backbone is represented by white ribbons, and the side chains (residues 100, 106, 181, and 229) are represented by colored wire style. AmBBU is represented by magenta wire style. Dotted lines show the interactions between HIV-1 RT and AmBBU. A D2 representation of the interactions is presented below the docking.

occur in the hydrophobic inhibitor-binding pocket of RT, which includes the residue Y181 (46). A single mutation in this pocket can lead to high-level resistance to earlier NNRTIs, including EFV and NVP. However, two or more mutations are required to cause high-level resistance to ETR, RPV, and other recent NNRTIs (3, 35, 53, 61). Y181C alone can cause multidrug resistance to NNRTIs, such as high-level resistance to NVP and DLV, and low-level resistance to EFV (18). In addition, Y181C provides the mutational foundation for the development of higher levels of ETR resistance (49). The Y181C mutation has emerged as an initial mutation in previous studies in patients failing an NNRTI-containing regimen, including NVP monotherapy (15, 43) and DLV monotherapy (17). K103N is frequently observed among NNRTI resistance mutations, but it is usually followed by Y181C and G190A (27). Resistance to HEPT derivatives is generated by mutations at multiple sites in the HIV-1 RT (8), while 1-(3-cyclopenten-1-yl)methyl-6-(3,5-dimethylbenzoyl)-5-ethyl-2,4-pyrimidinedione (SJ-3366) selected for a virus with the mutation Y181C after five tissue culture passages (9). In the present study, the initial mutation Y181C was sufficient for the acquisition of HIV-1 resistance to AzBBU and AmBBU. Other common NNRTI resistance mutations, such as K101E, K103N, and Y188C, were not identified.

Using docking studies, we examined the binding sites for the metabolically relevant derivative AmBBU on the allosteric pocket of HIV-1 RT (Fig. 4). According to the docking, AmBBU binds the allosteric pocket through arene-H interactions with the amino acid residues Leu100, Val106, Tyr181, and Trp229 (Fig. 4A). When the RT mutant Y181C was used for docking, AmBBU lost the interaction at position 181 (Fig. 4B). The docking score between HIV-1 RT (wt) and AmBBU was higher than that between HIV-1 RT (Y181C) and AmBBU, indicating the importance of the residue Tyr181 in the binding to the allosteric pocket. Most NNRTIs are engaged in the H-bond with the backbone of the residues Lys101 and/or Lys103 of RT (13, 26, 41). Previous docking studies suggested an H-bond between the amide of Lys101 and nitrogen of the cyanomethyl and picolyl group of 1-substituted 3-(3,5-dimethylbenzyl)uracils (33). In our previous study, we showed that 6-subtitutions on the uracil ring resulted in elevation of the anti-HIV-1 activity of the uracil derivatives (28). The structure-activity relationship among these uracil derivatives suggested that the strong anti-HIV-1 activity of the 6-amino derivative AmBBU is due to the H-bond formed between the 6-amino group of AmBBU and the amide group of the residue Lys101, as well as hydrophobic interactions (28). Here, our docking showed

TABLE 3 NNRTI-resistant mutations in the polymerase domain and amino acid changes in the RNase H domain of escape virus

		RT domain[a]								
		Polymerase					RNase H			
GenBank accession no.	Name	A98	K102	K103	V179	Y181	K451	R461	T468	D471
A04321	IIIB LAI	–	–	–	–	–	–	–	P	–
A07867	LAI-J19	–	–	–	–	–	–	–	–	–
AB221005	Ba-L	Q	–	–	–	–	–	–	S	–
AF033819	HXB2_copy LAI	–	–	–	–	–	–	–	–	–
AF070521	NL43E9 LAI IIIB_NY5	–	Q	–	–	–	–	–	P	–
D86068	MCK1 LAI IIIB	–	–	–	–	–	R	K	P	N
D86069	PM213 LAI IIIB	–	–	–	–	–	–	–	–	–
EU541617	pIIIB	–	Q	–	–	–	–	–	P	–
HB388803	MN patent seq	–	–	–	–	–	–	–	S	–
K02007	SF2 LAV2 ARV2	–	–	–	–	–	–	–	S	–
K02013	LAI BRU	–	–	–	–	–	–	–	–	–
K02083	PV22 LAI IIIB	–	–	–	–	–	R	K	P	N
K03455	HXB2-LAI-IIIB-BRU	–	–	–	–	–	–	–	–	–
M17449	MNCG MN	–	–	–	–	–	–	–	S	–
NC_001802	HXB2-LAI-HXB2R	–	–	–	–	–	–	–	–	–
U26942	NL4_3 LAI_NY5 pNL43 NL43	–	Q	–	–	–	–	–	P	–
U63632	JRFL JR_FL	–	–	R	I	–	–	–	S	–
X01762	REHTLV3 LAI IIIB	–	–	–	–	–	–	K	P	N
JQ070415	AzBBU IIIB-AZ	–	–	–	–	C	R	K	P	N
JQ070416	AmBBU IIIB-AM	–	–	–	–	C	R	K	P	N

[a] The default amino acids and position numbers are specified in each column subheading. –, No change.

arene-H interactions of AmBBU with Leu100, Val106, Tyr181, and Trp229 (Fig. 4A). However, we could not identify the precise role of the 6-amino substitution in the binding to the allosteric pocket and how it leads to an increased anti-HIV-1 activity. Thus, although several interactions occur within the allosteric pocket, the interaction with the Tyr181 residue appears essential for docking of 6-substituted 1-benzyl-3-(3,5-dimethylbenzyl)uracils. In addition, Y181C loses important aromatic ring interactions in the core of the NNRTI-binding pocket, decreasing binding of NNRTIs (42). Taken together, the results of sequence analysis and docking studies indicate that AmBBU requires the interaction(s) with Tyr181 for its inhibitory effect on HIV-1.

In addition to Y181C, we identified four mutations in the RNase H domain of RT: K451R, R461K, T468P, and D471N (Fig. 3). Since we do not know exactly when these mutations emerged in relation to Y181C, it is difficult to elucidate their precise role in acquisition of HIV-1 resistance to AzBBU and AmBBU. One possibility is that mutations in the RNase H domain are merely the result of polymorphisms of RT and are not related to Y181C, as indicated by several HIV-1 (subtype B) prototype strains containing some of the identified mutations in the RNase H domain (Table 3). The strains MCK1_LAI_III_B and PV22_LAI_III_B, for instance, display all four amino acid changes but are not associated with any common NNRTI-resistant mutation. However, some strains display one or more NNRTI-resistant mutations in association with the mutation T468P/S, suggesting that mutations in the RNase H domain could act in coordination with NNRTI-resistant mutations to favor drug resistance. It has been postulated that drug resistance mutations reduce the replication fitness of HIV-1 (10). NNRTI-resistant RTs with the Y181C mutation have been shown to alter the rate of one or both modes of RNase H cleavage with no significant effects on RNA- or DNA-dependent DNA polymerization, and a decrease in RNase H activity has been associated with greater reductions in replication fitness (2).

In 2005, Nikolenko et al. suggested that mutations in the RNase H domain could significantly contribute to an increase of RT resistance to NRTIs (37). Later, the same group proposed the RNase H-dependent NNRTI-resistant model, which suggests that mutations in the RNase H domain that reduce RNase H cleavage will allow more time for the NNRTIs to dissociate from the NNRTI-RT-template/primer complex, allowing the reinitiation of polymerization and thereby resulting in enhanced NNRTI resistance (36). Thus, combining mutations in RT that reduce NNRTI affinity with mutations that reduce RNase H cleavage should further increase NNRTI resistance (24, 36). In an RNase H-independent mechanism, NNRTIs themselves can increase RNase H activity, so that mutations reducing RNase H activity are selected in response to NNRTI therapy, because they restore the balance between RNase H activity and polymerization (16). An alternative explanation is that NNRTIs may inhibit HIV-1 replication by increasing RT dimer stability (51). Thus, NNRTI-binding pocket mutants that confer drug resistance should decrease the stability of RT heterodimers. In general, the nucleic acid structure-dependent interplay between polymerase and RNase H domains is likely to affect overall efficacy of NNRTIs against HIV-1 replication, as well as the selection of mutations in the NNRTI-binding site associated with NNRTI resistance.

The effects of mutations in the RNase H domain on NNRTI resistance have been confirmed *in vitro*, and yet their clinical impact is still unclear. Current HIV-1 genotypic analyses of patients generally focus on the N terminus of the polymerase domain, thus missing important information on mutations in the thumb-connection subdomains and RNase H domain that might be related to resistance either alone or in combination with other RT mutations. Yap et al. showed that N348I in the connection subdomain was highly prevalent in a patient cohort and was highly associated with thymidine analogue-associated mutations (TAMs) and the NNRTI mutations K103N and Y181C (59). Hachiya et al. also

examined N348I in treatment-experienced clinical isolates from Japan and found that N348I was prevalent in AZT and/or ddI therapy and that several mutations in the connection subdomain and RNase H domain typically acted as pretherapy polymorphisms (20, 21). Waters et al. found N348I prevalent in treatment-experienced patients (54). In addition, these researchers found that the genotypic profiles of patients with or without the K451R mutation within a treatment-experienced group showed a higher incidence of NNRTI mutations in patients with the K451R mutation. Santos et al. analyzed 450 sequences from Brazilian subtype B isolates and public databases and found nine mutations in the connection subdomain and six mutations in the RNase H domain that were associated with NRTI therapy (45). Positions K451 and D471 were less conserved in NRTI-experienced patients, while R461 and T468 were equally variable in both naive and experienced patients. A comparison of RNase H sequences in naive versus NRTI-experienced patients in a French cohort showed that mutations L469T/I/M/H, T470P/S/E/K, A554T/L/K, and K558R/G/E were more prevalent among treatment-experienced patients (44). However, Ntemgwa et al. analyzed RNase H mutations in NRTI-experienced patients from a Canadian and an Italian cohort and found positions D460, P468, H483, K512, and S519 to be extensively polymorphic in both naive and experienced patients (38). Recently, an analysis of patient sequences from databases showed that several mutations in the connection subdomain were significantly higher for sequences that contained one or more RTI resistance mutations compared to sequences without RTI resistance mutations (16). Moreover, subtype B-infected patient database analysis showed that RNase H mutations, including K451R, increased in frequency with the number of TAMs in a dose-dependent fashion (31). That study demonstrated that distinct RT C-terminal mutations can act as primary or secondary drug resistance mutations and are associated in a complex array of phenotypes with RT polymerase domain mutations.

In this *in vitro* study, we identified four mutations in the RNase H domain that might be related to the NNRTI resistance mutation Y181C. Biochemical studies are needed to understand the molecular mechanism of the associations and interactions between mutations within the polymerase and RNase H domains of RT. Further experiments are under consideration to validate the role of these mutations in the acquisition of resistance to AzBBU and AmBBU. First, viral strains containing the identified mutations in the RNase H domain, such as MCK1_LAI_IIIB and PV22_LAI_IIIB, will be used for testing the uracil derivatives, since these strains have all four amino acid changes but are not associated with any common NNRTI-resistant mutation. Second, recombinant RT enzymes containing the identified mutations will be used to determine the inhibitory effects of AzBBU and AmBBU on their catalytic activity. Third, an experiment on site-directed mutagenesis will be performed to elucidate the precise role of the RNase H mutations in the acquisition of resistance.

In terms of drug development, we found useful information for the future design of 6-substituted uracil derivatives with enhanced chemical properties that improve anti-HIV-1 activity and resistance profiles. Although the chemical properties of AzBBU and AmBBU suggest a good drug-likeness profile, further studies are required to assess the toxicity and pharmacokinetics of 6-substituted uracil derivatives *in vivo*. A limitation of our study relates to the use of laboratory strains. However, the mutations that we identified have been reported in clinical isolates (38, 45, 54). Another limitation of our study relates to the lack of information on the mutations in the RNase H domain of NNRTI-treated patients, since these mutations have been reported mostly in NRTI-treated patients. Furthermore, in a clinical setting, NNRTIs must be used in combination therapy, which may alter the pattern for resistance. Thus, the emergence of drug resistance should be further investigated and confirmed in clinical trials.

In conclusion, our results provide important information on the acquisition of resistance to the novel uracil derivatives AzBBU and AmBBU. Although the initial mutation Y181C can be sufficient in the acquisition of HIV-1 resistance, additional mutations in the RNase H domain of RT could additionally be associated to the mechanisms of resistance. Docking studies using the crystal structure of RT showed that AmBBU requires the amino acid residues Leu100, Val106, Tyr181, and Trp229 for its inhibitory effect on HIV-1. Further studies are necessary to determine the precise role of each mutation in the acquisition of HIV-1 resistance to the present compounds.

ACKNOWLEDGMENT

This study was supported in part by a research grant from the Ministry of Health, Labor, and Welfare of Japan.

REFERENCES

1. **Agarwal AK, Fishwick CW.** 2010. Structure-based design of anti-infectives. Ann. N. Y. Acad. Sci. **1213**:20–45.
2. **Archer RH, et al.** 2000. Mutants of human immunodeficiency virus type 1 (HIV-1) reverse transcriptase resistant to nonnucleoside reverse transcriptase inhibitors demonstrate altered rates of RNase H cleavage that correlate with HIV-1 replication fitness in cell culture. J. Virol. **74**:8390–8401.
3. **Azijn H, et al.** 2010. TMC278, a next-generation nonnucleoside reverse transcriptase inhibitor (NNRTI), active against wild-type and NNRTI-resistant HIV-1. Antimicrob. Agents Chemother. **54**:718–727.
4. **Baba M, et al.** 1991. Potent and selective inhibition of human immunodeficiency virus type 1 (HIV-1) by 5-ethyl-6-phenylthiouracil derivatives through their interaction with the HIV-1 reverse transcriptase. Proc. Natl. Acad. Sci. U. S. A. **88**:2356–2360.
5. **Baba M, et al.** 1994. Preclinical evaluation of MKC-442, a highly potent and specific inhibitor of human immunodeficiency virus type 1 *in vitro*. Antimicrob. Agents Chemother. **38**:688–692.
6. **Balzarini J, Karlsson A, De Clercq E.** 1993. Human immunodeficiency virus type 1 drug-resistance patterns with different 1-[(2-hydroxyethoxy)methyl]-6-(phenylthio)thymine derivatives. Mol. Pharmacol. **44**:694–701.
7. **Boyer PL, Currens MJ, McMahon JB, Boyd MR, Hughes SH.** 1993. Analysis of nonnucleoside drug-resistant variants of HIV-1 reverse transcriptase. J. Virol. **67**:2412–2420.
8. **Buckheit RW, Jr, et al.** 1995. Resistance to 1-[(2-hydroxyethoxy) methyl]-6-(phenylthio)thymine derivatives is generated by mutations at multiple sites in the HIV-1 reverse transcriptase. Virology **210**:186–193.
9. **Buckheit RW, Jr, et al.** 2001. SJ-3366, a unique and highly potent non-nucleoside reverse transcriptase inhibitor of human immunodeficiency virus type 1 (HIV-1) that also inhibits HIV-2. Antimicrob. Agents Chemother. **45**:393–400.
10. **Coffin JM.** 1995. HIV population dynamics *in vivo*: implications for genetic variation, pathogenesis, and therapy. Science **267**:483–489.
11. **Coffin JM, Hughes SH, Varmus HE.** 1997. Retroviruses. Cold Spring Harbor Laboratory Press, New York, NY.
12. **Corbau R, et al.** 2010. Lersivirine, a nonnucleoside reverse transcriptase inhibitor with activity against drug-resistant human immunodeficiency virus type 1. Antimicrob. Agents Chemother. **54**:4451–4463.
13. **Das K, Jr, et al.** 2004. Roles of conformational and positional adaptability in structure-based design of TMC125-R165335 (etravirine) and related non-nucleoside reverse transcriptase inhibitors that are highly potent and effective against wild-type and drug-resistant HIV-1 variants. J. Med. Chem. **47**:2550–2560.
14. **De Clercq E.** 1993. HIV-1-specific RT inhibitors: highly selective inhibi-

tors of human immunodeficiency virus type 1 that are specifically targeted at the viral reverse transcriptase. Med. Res. Rev. 13:229–258.
15. **Delaugerre C, et al.** 2001. Resistance profile and cross-resistance of HIV-1 among patients failing a non-nucleoside reverse transcriptase inhibitor-containing regimen. J. Med. Virol. 65:445–448.
16. **Delviks-Frankenberry KA, Nikolenko GN, Pathak VK.** 2010. The "connection" between HIV drug resistance and RNase H. Viruses 2:1476–1503.
17. **Demeter LM, et al.** 2000. Delavirdine susceptibilities and associated reverse transcriptase mutations in human immunodeficiency virus type 1 isolates from patients in a phase I/II trial of delavirdine monotherapy (ACTG 260). Antimicrob. Agents Chemother. 44:794–797.
18. **Fontaine E, Vaerenbergh KV, Vandamme AM, Schmit JC.** 1999. Multidrug resistant human immunodeficiency virus type 1. AIDS Rev. 1:231–237.
19. **Goto J, Kataoka R, Muta H, Hirayama N.** 2008. ASEDock-docking based on alpha spheres and excluded volumes. J. Chem. Infect. Model. 48:583–590.
20. **Hachiya A, et al.** 2008. Amino acid mutation N348I in the connection subdomain of human immunodeficiency virus type 1 reverse transcriptase confers multiclass resistance to nucleoside and nonnucleoside reverse transcriptase inhibitors. J. Virol. 82:3261–3270.
21. **Hachiya A, et al.** 2009. Clinical relevance of substitutions in the connection subdomain and RNase H domain of HIV-1 reverse transcriptase from a cohort of antiretroviral treatment-naive patients. Antivir. Res. 82:115–121.
22. **Halgren TA.** 1999. MMFF VI. MMFF94s option for energy minimization studies. J. Comput. Chem. 20:720–729.
23. **Halgren TA.** 1999. MMFF VII. Characterization of MMFF94, MMFF94s, and other widely available force fields for conformational energies and for intermolecular-interaction energies and geometries. J. Comput. Chem. 20:730–748.
24. **Hang JQ, et al.** 2007. Substrate-dependent inhibition or stimulation of HIV RNase H activity by non-nucleoside reverse transcriptase inhibitors (NNRTIs). Biochem. Biophys. Res. Commun. 352:341–350.
25. **Haraguchi K, et al.** 2003. Synthesis of a highly active new anti-HIV agent 2′,3′-didehydro-3′-deoxy-4′-ethynylthymidine. Bioorg. Med. Chem. Lett. 13:3775–3777.
26. **Hopkins AL, et al.** 1996. Complexes of HIV-1 reverse transcriptase with inhibitors of the HEPT series reveal conformational changes relevant to the design of potent non-nucleoside inhibitors. J. Med. Chem. 39:1589–1600.
27. **Ibe S, Sugiura W.** 2011. Clinical significance of HIV reverse-transcriptase inhibitor-resistance mutations. Future Microbiol. 6:295–315.
28. **Isono Y, et al.** 2011. Synthesis of 1-benzyl-3-(3,5-dimethylbenzyl)uracil derivatives with potential anti-HIV activity. Antivir. Chem. Chemother. 22:57–65.
29. **Johnson VA, et al.** 2006. Update of the drug resistance mutations in HIV-1: Fall 2006. Top. HIV Med. 14:125–130.
30. **Klibanov OM, Kaczor RL.** 2010. IDX-899, an aryl phosphinate-indole non-nucleoside reverse transcriptase inhibitor for the potential treatment of HIV infection. Curr. Opin. Invest. Drugs 11:237–245.
31. **Lengruber RB, et al.** 2011. Phenotypic characterization of drug resistance-associated mutations in HIV-1 RT connection and RNase H domains and their correlation with thymidine analogue mutations. J. Antimicrob. Chemother. 66:702–708.
32. **Lightfoote MM, et al.** 1986. Structural characterization of reverse transcriptase and endonuclease polypeptides of the acquired immunodeficiency syndrome retrovirus. J. Virol. 60:771–775.
33. **Maruyama T, et al.** 2006. Synthesis and anti-HIV-1 and anti-HCMV activity of 1-substituted 3-(3,5-dimethylbenzyl)uracil derivatives. Chem. Pharm. Bull. 54:325–333.
34. **Maruyama T, et al.** 2003. Synthesis and antiviral activity of 1,3-disubstituted uracils against HIV-1 and HCMV. Antivir. Chem. Chemother. 14:271–279.
35. **Moyle G, et al.** 2010. Phase 2a randomized controlled trial of short-term activity, safety, and pharmacokinetics of a novel nonnucleoside reverse transcriptase inhibitor, RDEA806, in HIV-1-positive, antiretroviral-naive subjects. Antimicrob. Agents Chemother. 54:3170–3178.
36. **Nikolenko GN, Delviks-Frankenberry KA, Pathak VK.** 2010. A novel molecular mechanism of dual resistance to nucleoside and nonnucleoside reverse transcriptase inhibitors. J. Virol. 84:5238–5249.
37. **Nikolenko GN, et al.** 2005. Mechanism for nucleoside analog-mediated abrogation of HIV-1 replication: balance between RNase H activity and nucleotide excision. Proc. Natl. Acad. Sci. U. S. A. 102:2093–2098.
38. **Ntemgwa M, et al.** 2007. Variations in reverse transcriptase and RNase H domain mutations in human immunodeficiency virus type 1 clinical isolates are associated with divergent phenotypic resistance to zidovudine. Antimicrob. Agents Chemother. 51:3861–3869.
39. **Pauwels R, et al.** 1988. Rapid and automated tetrazolium-based colorimetric assay for the detection of anti-HIV compounds. J. Virol. Methods 20:309–312.
40. **Ren J, et al.** 1995. High resolution structures of HIV-1 RT from four RT-inhibitor complexes. Nat. Struct. Biol. 2:293–302.
41. **Ren J, et al.** 2000. Structural basis for the resilience of efavirenz (DMP-266) to drug resistance mutations in HIV-1 reverse transcriptase. Structure 8:1089–1094.
42. **Ren J, et al.** 2001. Structural mechanisms of drug resistance for mutations at codons 181 and 188 in HIV-1 reverse transcriptase and the improved resilience of second generation non-nucleoside inhibitors. J. Mol. Biol. 312:795–805.
43. **Richman DD, et al.** 1994. Nevirapine resistance mutations of human immunodeficiency virus type 1 selected during therapy. J. Virol. 68:1660–1666.
44. **Roquebert B, et al.** 2007. Relationship between mutations in HIV-1 RNase H domain and nucleoside reverse transcriptase inhibitors resistance mutations in naive and pretreated HIV-infected patients. J. Med. Virol. 79:207–211.
45. **Santos AF, et al.** 2008. Conservation patterns of HIV-1 RT connection and RNase H domains: identification of new mutations in NRTI-treated patients. PLoS One 3:e1781.
46. **Sarafianos SG, et al.** 2009. Structure and function of HIV-1 reverse transcriptase: molecular mechanisms of polymerization and inhibition. J. Mol. Biol. 385:693–713.
47. **Smith JS, Roth MJ.** 1992. Specificity of human immunodeficiency virus-1 reverse transcriptase-associated ribonuclease H in removal of the minus-strand primer, tRNA(Lys3). J. Biol. Chem. 267:15071–15079.
48. **Spence R, Kati W, Anderson K, Johnson K.** 1995. Mechanism of inhibition of HIV-1 reverse transcriptase by non-nucleoside inhibitors. Science 267:988–993.
49. **Stanford University.** HIV drug resistance database: NNRTI resistance notes. Stanford University, Stanford, CA. http://hivdb.stanford.edu/cgi-bin/NNRTIResiNote.cgi.
50. **Szczech GM, et al.** 2000. Safety assessment, in vitro and *in vivo*, and pharmacokinetics of emivirine, a potent and selective nonnucleoside reverse transcriptase inhibitor of human immunodeficiency virus type 1. Antimicrob. Agents Chemother. 44:123–130.
51. **Tachedjian Orlova GM, Sarafianos SG, Arnold E, Goff SP.** 2001. Nonnucleoside reverse transcriptase inhibitors are chemical enhancers of dimerization of the HIV type 1 reverse transcriptase. Proc. Natl. Acad. Sci. U. S. A. 98:7188–7193.
52. **Tanaka H, et al.** 1995. Synthesis and antiviral activity of 6-benzil analogs of 1-[(2-hydroxyethoxy)methyl]-6-(phenylthio)thymine (HEPT) as potent and selective anti-HIV-1 drugs. J. Med. Chem. 38:2860–2865.
53. **Vingerhoets J, et al.** 2010. Resistance profile of etravirine: combined analysis of baseline genotypic and phenotypic data from the randomized, controlled Phase III clinical studies. AIDS 24:503–514.
54. **Waters JM, et al.** 2009. Mutations in the thumb-connection and RNase H domain of HIV type-1 reverse transcriptase of antiretroviral treatment-experienced patients. Antivir. Ther. 14:231–239.
55. **Weiner SJ, et al.** 1984. A new force field for molecular mechanical simulation of nucleic acids and proteins. J. Am. Chem. Soc. 106:765–784.
56. **Wilkin A, et al.** 17 October 2011. Long-term efficacy, safety and tolerability of rilpivirine (RPV, TMC278) in HIV type 1-infected antiretroviral-naive patients: week 192 results from a phase IIb randomized trial. AIDS Res. Hum. Retrovir. [Epub ahead of print].
57. **Witvrouw M, et al.** 1999. Activity of non-nucleoside reverse transcriptase inhibitors against HIV-2 and SIV. AIDS 13:1477–1483.
58. **Wohrl BM, Moelling K.** 1990. Interaction of HIV-1 ribonuclease H with polypurine tract containing RNA-DNA hybrids. Biochemistry 29:10141–10147.
59. **Yap SH, et al.** 2007. N348I in the connection domain of HIV-1 reverse transcriptase confers zidovudine and nevirapine resistance. PLoS Med. 4:e335.
60. **Zhan P, et al.** 2011. HIV-1 NNRTIs: structural diversity, pharmacophore similarity, and implications for drug design. Med. Res. Rev.. doi:10.1002/med.
61. **Zhou XJ, et al.** 2009. Single-dose escalation and multiple-dose safety, tolerability, and pharmacokinetics of IDX899, a candidate human immunodeficiency virus type 1 nonnucleoside reverse transcriptase inhibitor, in healthy subjects. Antimicrob. Agents Chemother. 53:1739–1746.

Bioorganic & Medicinal Chemistry Letters 22 (2012) 7742–7747

Contents lists available at SciVerse ScienceDirect

Bioorganic & Medicinal Chemistry Letters

journal homepage: www.elsevier.com/locate/bmcl

Structure based medicinal chemistry approach to develop 4-methyl-7-deazaadenine carbocyclic nucleosides as anti-HCV agent

Anandarajan Thiyagarajan [a], Mohammed T. A. Salim [b], Tuniki Balaraju [a], Chandralata Bal [a,*], Masanori Baba [b], Ashoke Sharon [a,*]

[a] Department of Applied Chemistry, Birla Institute of Technology, Mesra, Ranchi 835215, India
[b] Division of Antiviral Chemotherapy, Center for Chronic Viral Diseases, Graduate School of Medical and Dental Sciences, Kagoshima University, 8-35-1, Sakuragaoka, Kagoshima 890-8544, Japan

ARTICLE INFO

Article history:
Received 30 July 2012
Revised 16 September 2012
Accepted 19 September 2012
Available online 13 October 2012

Keywords:
Hepatitis C Virus
Carbocyclic nucleoside
Nucleoside inhibitor
Drug like properties
Molecular modelling

ABSTRACT

The structure-based approaches were implemented to design and rationally select the molecules for synthesis and anti-HCV activity evaluation. The systematic structure–activity relationships of previously discovered molecules (types **I**, **II**, **III**) were analyzed to design new molecules (type **IV**) by bioisosteric replacement of the amino group. The ligand conformation, binding mode studies and drug like properties were major determinant for selection of molecules for final synthesis. The replacement of amino group with methyl restored the interactions with RNA-template (Tem 799) through bifurcated weak H-bond (C–H...O). This is an interesting finding observed from molecular modeling studies. It was found that **6c–e** has anti-HCV activity (EC_{50} in 37–46 μM) while **6a, 6b** and **6g** were inactive. The compound **6f** (EC_{50} 28 μM) was the most active among the series however it also showed some cytotoxicity (CC_{50} 52.8 μM). Except **6f**, none of the compounds were found to be cytotoxic (CC_{50} > 100 μM). The present study discloses structure–based approach for novel anti-HCV lead discovery and opens a future scope of lead optimization.

Hepatitis C virus (HCV), a member of *Flaviviridae* family is now considered under major health threat with more than 200 million infected individuals worldwide.[1] In addition, long-term infection can lead to chronic liver disease, such as cirrhosis of the liver or hepatocellular carcinoma. Current standard therapy involving combination of interferon-alpha (IFN-α) and ribavirin has limited efficacy and is associated with significant side-effects even when used with the newly approved HCV protease inhibitors telaprevir and boceprevir. Therefore, there is a need for more effective anti-HCV agents that can be used in IFN-α/ribavirin sparing regimens.[2] An ideal therapy against hepatitis C is expected to have a broad spectrum of activity against all HCV genotypes, shorten treatment duration, minimal side effects and a high barrier to resistance. The HCV non-structural (NS) protein NS5B RNA-dependent RNA polymerase (RdRp) is a key component of the replicative complex and is responsible for initiating and catalyzing viral RNA synthesis.[3,4] Nucleoside analogues continue to play a vital role in the search for improved therapies for HCV infection. Nucleosides that target HCV RdRp have demonstrated advantages of broader activity against various HCV genotypes and a higher barrier to development of resistant viruses when compared to known HCV protease inhibitors.[5] The recent report on anti-HCV compound discloses various structural modifications of nucleosides either on sugar or on the base to discover new agents (Fig. 1) with improved efficacy and safety over existing drugs.[6–11]

Introduction of a 2′-CH_3 to the sugar ring of adenosine, the natural substrate, yielded highly potent type **I** molecule (Fig. 1).[8] Further, keeping the modification of sugar constant and applying bioisosteric replacement of 7-N with 7-CH generated equally or even more potent inhibitors (type **II** molecules).[8] An interesting induction of bioisosteric replacement of oxygen with methylene of sugar ring of type **II** resulted a new class of molecules (type **III**) recognized as carbocyclic nucleosides. This modification didn't show significant impact on biological profile but was able to maintain moderate activity. However, the glycosidic bond of carbocyclic nucleosides are resistant to nucleoside phosphorylase as well as nucleoside hydrolase and is more stable towards metabolic degradation in comparison to natural nucleoside.[12] Due to these features, carbocyclic nucleosides have received much attention as potential chemotherapeutic agents.[13–16]

These structure–activity (Fig. 1) understanding studies provided us a rational basis of structural modification to design newer analogs for better drug like profile. In the present investigation we have done bioisosteric replacement of the exocyclic amino group of type **III** with a methyl group to generate type **IV** molecules. From the various possible 7-substituted analogs, five were selected for

* Corresponding author.
E-mail addresses: cbal@bitmesra.ac.in (C. Bal), asharon@bitmesra.ac.in (A. Sharon).

0960-894X/$ - see front matter © 2012 Elsevier Ltd. All rights reserved.
http://dx.doi.org/10.1016/j.bmcl.2012.09.072

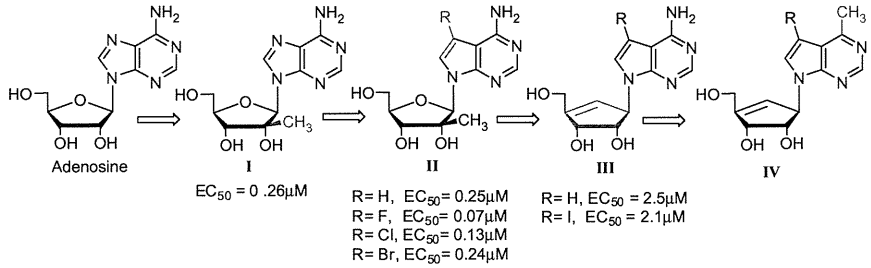

Figure 1. The chemical structure of newly discovered anti-HCV molecules (**I-III**). The arrow indicates stepwise modifications (indicated with red). Type **IV** is the prototype molecules designed and selected for present investigation.

synthesis on basis of a novel approach using conformational fundamental of nucleoside analogs in free-state as well as in receptor-complex.

We have recently developed the catalytic model of HCV RdRp complex[17] using the apo structure (1gx6) of HCV RdRp. The model structure comprises the complex with short template-primer chain along with the two metal ions (Fig. 2a).

The template, primer and metal ions has been extracted from published crystal structure of HIV-RT[18] to incorporate into HCV RdRp utilizing the information from recently published crystal structure of HCV RdRp complex.[19] The HCV RdRp-ATP interaction mode was more closely studied (Fig. 2b) and its understanding was imposed to our designed molecules (type **IV**) to select final molecules for synthesis. The Figure. 2b shows base pairing with template (black block: Tem799) by hydrogen bond (pink dotted line). Two metal ions MG699 and MG599 interact via metal coordinate bond (gray solid line) with Pα and Pγ phosphate respectively. The triphosphate motif was found to strongly held by polar residues Arg158, Arg48, and Lys51 through H-bonding (pink solid line and pink dotted line). The triad of aspartic acid (Asp318, Asp319 and Asp225) was found close to Pα and sugar motif of ATP. Asp 225 forms H-bonding with 3′-OH of sugar ring. The hydrophobic residues Gly 317, Phe 193, Phe 224, Cys 223, Ile 160 were found to closely associated with ATP binding. Further, hydrophilic residues Ser 288, Thr 287, Asn 291, Asn 316, Thr 221 and Ser 282 were also observed to closely interact with ATP.

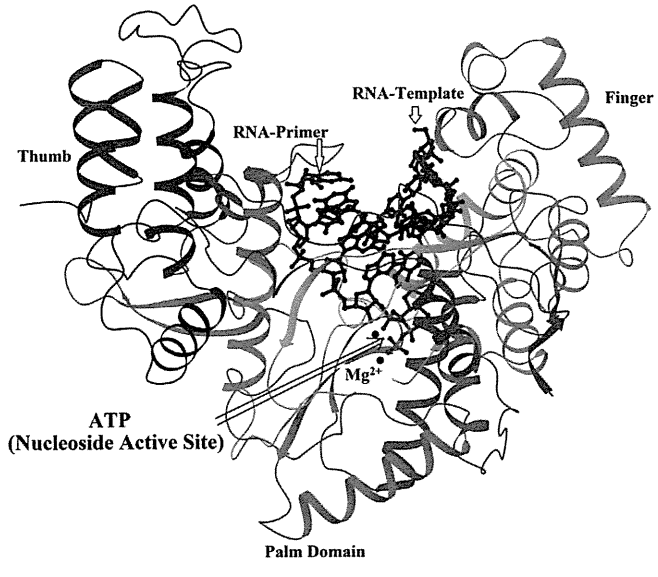

Figure 2a. A model structure of HCV RdRp with RNA double strand (primer and template), adenosine triphosphate (ATP) and two metal ions, highlighting the position of nucleoside active site.

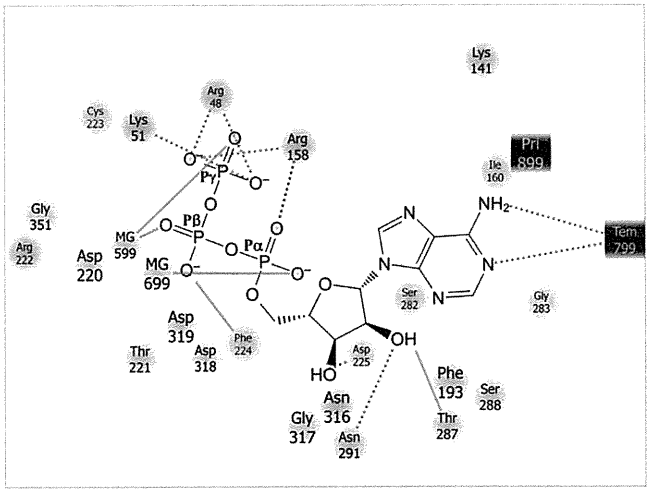

Figure 2b. Interaction profiles of ATP with HCV RdRp.

Most of the antiviral nucleoside analogs are metabolized to the corresponding nucleoside 5′-triphosphate by cellular enzymes to behave as alternative substrates for the viral polymerase followed by the nucleic acid chain termination. Therefore the modelling calculations were conducted on triphosphate form of natural substrate (adenosine) as well as our designed molecules.

The structural study of HCV RdRp-ATP complex (Fig. 3a) defines the key point related to molecular recognition motif of nucleoside binding; (i) two metal ions (Mg^{2+}) placement by interaction with Asp 220, Asp 318 and triphosphate motif of ATP; (ii) triphosphate motif conformationally positioned through H-bonding mediated by basic residues (Arg 48, Lys 51 and Arg 158); (iii) interaction of one of the Mg^{2+} with 3′-OH of primer and Pα possibly catalyzes viral RNA (vRNA) elongation through formation of 3′-O...Pα bond; (iv) HCV RdRp complex is stabilized by formation of π...π stacking (RNA primer) and strong H-bonding (pink dotted line, RNA template) between incoming nucleotide (here ATP); (v) ATP was found to be in 2′-exo conformation along with anti-disposition of base, forming H-bond pairing with RNA-template describes the importance of anti-conformation of nucleoside. Thus, the discussed features were considered as the basic recognition requirement to analyze newly designed molecules. We started with analyzing the conformations of designed molecules at nucleoside level. The conformational search was carried out for the designed molecules and top conformer was chosen for superposition with adenosine. Figure 3b shows the conformational analysis of **6a** (shown in brown), which satisfy the critical conformational requirement of molecules to fit into the nucleoside active site. Overall the main conformational feature such as anti base-disposition and 2′-exo were found significantly same for **6a** in comparison to natural substrate (adenosine: natural atom colour), however the marginal difference were observed in 5′-OH and 4′-puckering.

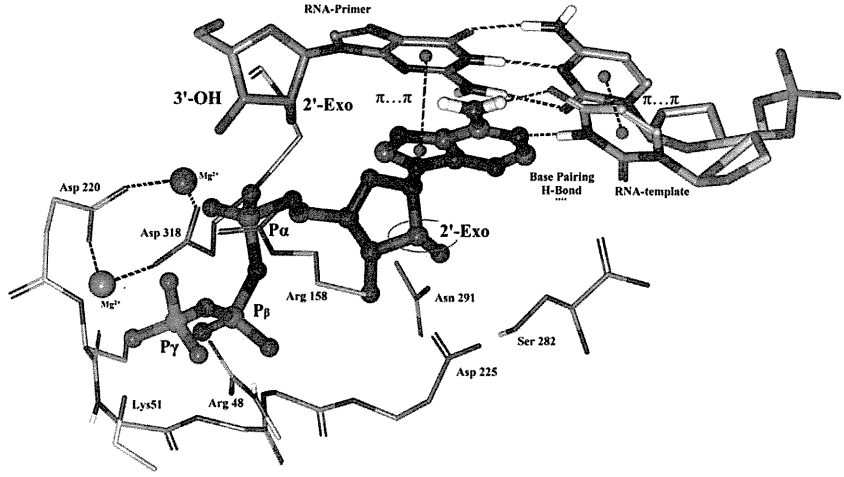

Figure 3a. HCV RdRp complex shows the binding mode of ATP and highlights the major catalytic non-covalent interaction profiles.

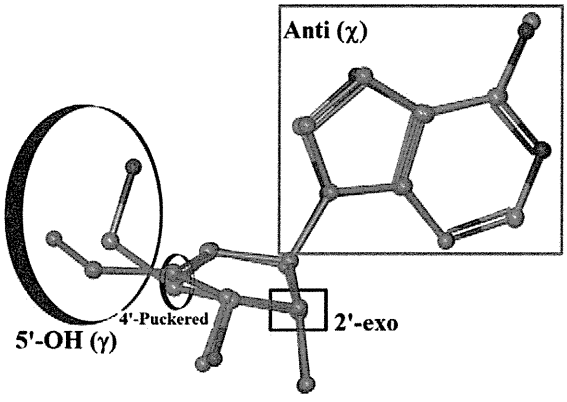

Figure 3b. The superposition of top conformation of adenonsine (natural atom colour) and **6a** (brown).

Conformational and superposition analysis for rest of the molecules were done similarly and selected molecules (Table 1) were further analyzed by molecular docking of their triphosphate form to understand the binding mode. The electrostatic surface diagram and docked complex for triphosphates were generated to investigate the possibility to fit into the nucleoside active site of HCV RdRp. Figs. 4a and 4b shows electrostatic surface and docked complex diagram for **6e** respectively.

It is evident from Figure 4a that the triphosphate motif occupies the basic cavity (blue), the base motif and carbocyclic sugar fits near to RNA, where a mixed pattern of acidic and hydrophobic surfaces were found. The interaction figure (Fig. 4b) highlights the major non-covalent interactions similar to previously discussed binding profile of ATP (see Fig. 3a). As the 7-NH_2 is replaced with a methyl group in **6e**, the strong H-bonding with RNA-template (Tem 799) was lost. However, the methyl group was able to form a bifurcated weak H-bond (C–H...O) with template. This is an interesting finding observed from molecular docking studies. Only X-ray crystal structure of designed molecule with HCV RdRp can help to confirm this observation, which is beyond the scope of current manuscript.

Glide[20] of Schrodinger Suite[21] was used for molecular docking to investigate the binding mode and docking score. Overall the docking score (Table 1), conformational similarities (Figs. 3b and 4a) and binding mode (Fig. 4b) were chosen as major rational for selection of molecules for synthesis and anti-HCV activity evaluation. The drugs like properties (DLP) were estimated using QikProp

Table 1
In-silico binding analysis and drug like properties (DLP) of analogs selected for synthesis

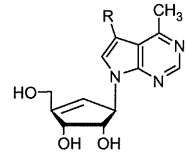

R	Molecular docking Score[a]	MM-GBSA score[b]	DLP violation[c]	
	Glide score[a]	DG	#5[d]	#3[e]
H	−12.15	−125.8	0	0
F	−13.54	−121.2	0	0
Cl	−13.56	−134.6	0	0
Br	−13.57	−132.4	0	0
I	−13.64	−130.8	0	0
$-CH{=}CH_2$	−13.53	−125.8	0	0
$-C{\equiv}CH$	−13.73	−125.6	0	0

[a] Glide score (G-score): The minimized poses are rescored using Schrödinger's proprietary GlideScore scoring function and the binding affinity can be estimated by G-score.

[b] MM-GBSA Score: DG = *E*_complex(minimized) − [*E*_ligand (from minimized complex) + *E*_receptor]; DG is the ligand/receptor interaction energy of the complex.

[c] DLP: Drug Like Properties.

[d] #5: Number of violations of Lipinski's rule of five. The rules are: molecular weight MW <500, QPlogPo/w <5, donorHB ⩽5, accptHB ⩽10. Compounds that satisfy these rules are considered drug-like.

[e] #3: Number of violations of Jorgensen's rule of three. The three rules are: QPlog*S* > −5.7, QPPCaco >22 nm/s, primary metabolites <7. Compounds with fewer violations of these rules are more likely to be orally available.

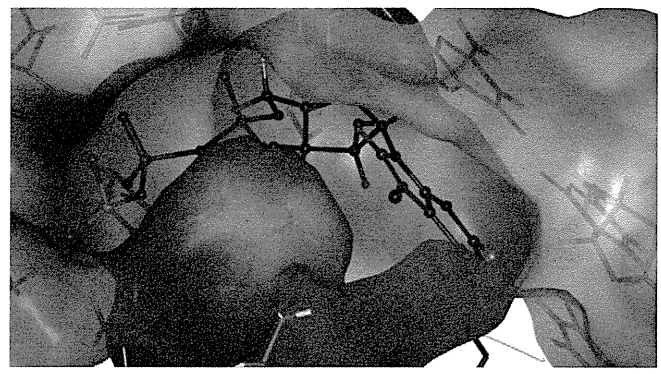

Figure 4a. The electrostatic surface diagram showing the binding of triphosphate of **6e** into the nucleoside active site.

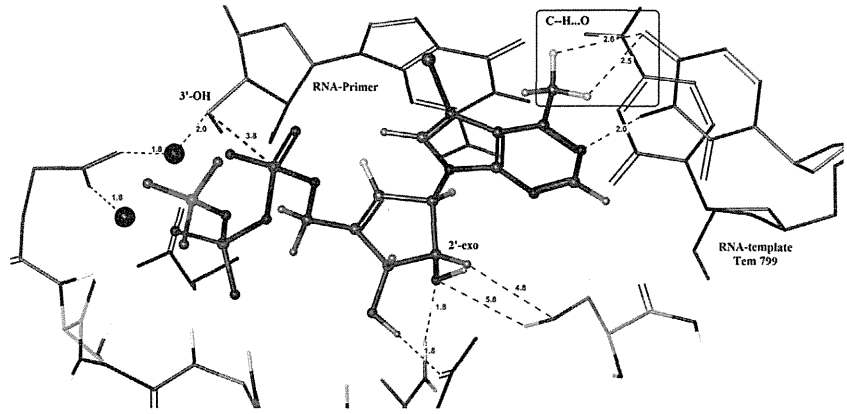

Figure 4b. The docked complex of **6e** into HCV RdRp showing a detail binding profile.

module of Schrödinger Software Suite for the selected molecules (Table 1). None of the molecules violated Lipinski's rule[22] of five as well as Jorgensen's rule[23,24] of three. Thus, the present modelling studies support the selection of analogs for final synthesis

The modified carbocyclic sugar (**1**) as a single isomer, was prepared as per earlier reported procedure[25] in eight steps from commercially available D-ribose with some optimization. During, trityl protection, DCM and DMF mixture (4:1) was used in place of DMF, which reduced the reaction time from 48 h to 12 h and made work up easier. In the TBS protection step, DMAP was used in catalytic amount using single solvent DCM. Thus, the improved procedure was able to provide 15% overall purified yield of carbocyclic sugar key intermediate **1** starting from D-ribose (Scheme 1). The optical rotation of **1** was found to be +30.9 ($[\alpha]_D^{29}$), which is close to the reported value of +28.4 ($[\alpha]_D^{23}$).[26]

4-Chloro-7*H*-pyrrolo[2,3-*d*]pyrimidine (**2**) was purchased from CiVenti Chem (India) Private Limited. The cross coupling reaction strategy[27] was applied using trimethylaluminium and $Pd(Ph_3P)_4$ catalysis to generate 4-methyl-7*H*-pyrrolo[2,3-*d*]pyrimidine (3a, Scheme 2). The Cl/Br/I was successfully introduced at C-7 of **3a** through reaction with respective *N*-halosuccinimide in DMF to generate **3c–e**. The introduction of fluoro group was a three step procedure. In brief, **2** was first treated with *N*-bromosuccinimide to introduce bromo group at C-7 (**4**), which was replaced with fluoro (**5**) by reaction with NFSI and *n*-BuLi followed by cross coupling with trimethylaluminium to yield **3b**.

Mitsunobu coupling of **1** with **3a–e** yielded protected coupled products, which were isolated, purified and deprotected to yield desired final compounds **6a–e** (Scheme 3).[28] Heck reaction was utilized for the synthesis of **6f**[29] and **6g**[30] as described in Scheme 4 with modification to earlier reported procedure.[10] In brief, **6e** was utilized as starting aryl halide and tributylvinyltin (for **6f**) or trimethylsilylacetylene (for **6g**) to introduce vinyl or ethyne group respectively.

Reaction of tributyltin directly yielded the desired product while reaction of trimethylsilylacetylene yielded the trimethylsilylated derivative, which was purified and deprotected by stirring with K_2CO_3 in methanol at room temperature.

The anti-HCV assay of **6a–g** was carried out in subgenome HCV RNA replicon cells containing the luciferase gene. The anti-HCV activity of compounds was determined by reduction of luciferase activity, while the cytotoxicity was evaluated by a tetrazolium dye method. From the dose-dependent study results (data not shown), EC_{50} (50% effective concentration) and CC_{50} (50% cytotoxic

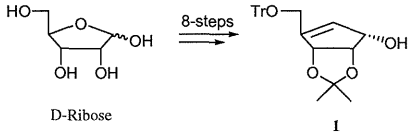

Scheme 1. Synthetic strategy for the preparation of carbocyclic sugar key intermediate **1** from D-ribose.

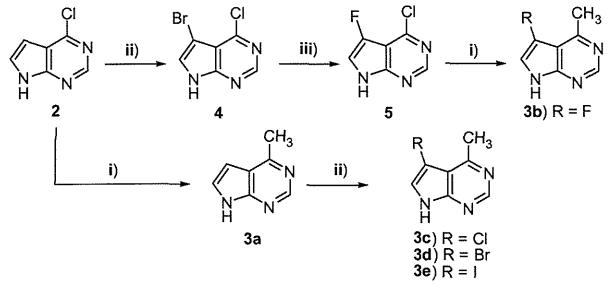

Scheme 2. Reagents and conditions: (i) $Pd(Ph_3P)_4$, $Al(CH_3)_3$, THF, 75 °C, 8 h; (ii) *N*-halosuccinimide, DMF, rt, 10 h; (iii) *n*-BuLi, NFSI, THF, −78 °C, 2 h.

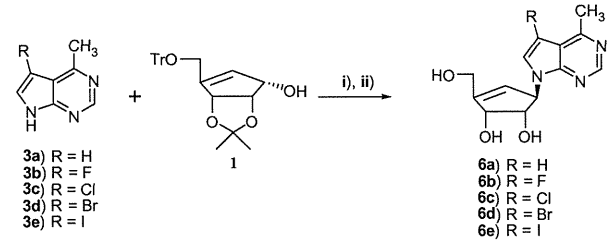

Scheme 3. Reagents and conditions: (i) Ph_3P, DIAD, THF, 0–5 °C, 2 h; (ii) 10% HCl in CH_3OH, 60 °C, 5 h.

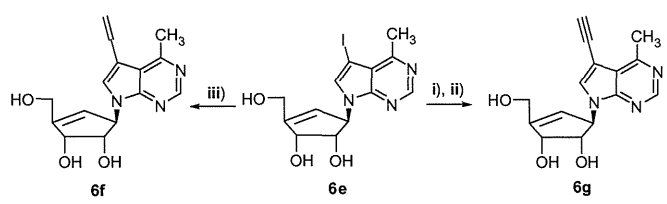

Scheme 4. Reagents and conditions: (i) $Pd(PPh_3)_4$, CuI, trimethylsilylacetylene, Et_3N, DMF, rt, 10 h; (ii) K_2CO_3, CH_3OH, rt, 4 h; (iii) $Pd(PPh_3)_4$, CuI, tributylvinyltin, Et_3N, DMF, 50 °C, 6 h.

Table 2
Anti-HCV activity of synthesized compounds

Compound	EC_{50}[b] in μM	CC_{50}[a] in μM
6a	> 100	>100
6b	> 100	> 100
6c	41.7	>100
6d	37.3	>100
6e	46.2	>100
6f	28.0	52.8
6g	67.7	>100
KZ-16	0.17	> 10

[a] The 50% cytotoxic concentration, determined by the reduction of viable cell number.
[b] The 50% effective concentration, determined by the inhibition of luciferase activity.

concentration) were calculated, and they are summarized in Table 2. KZ-16 was used as a reference compound, which has been recently reported to have selective anti-HCV activity.[31]

From the results, it was found that **6c–e** have some anti-HCV activity (Fig. 5) while **6a**, **6b** and **6g** were inactive. The compound **6f** was the most active among the series; however it also showed significant cytotoxicity. Except for **6f**, none of the compounds were found to be cytotoxic with CC_{50} values >100 μM.

Most of the molecular modeling studies were conducted on updated version of Schrödinger suite.[21] The first unliganded structure of HCV polymerases has been published[32] in 1999. Later crystal structure studies[33] with nucleoside triphosphate (NTP) form of natural substrate revealed the presence of conserved aspartic acids along with the catalytic Mg^{2+} ion (di-metal ion mechanism)[34] in the active site. The findings were previously seen in the crystal structure of HIV-RT.[18] The Prime[35] module has been used to built the model structure of HCV RdRp complex[17] using apo structure (pdb: 1gx6)[32] and HCV RdRp crystal structure (pdb: 4E7A).[19] The template, primer and metal ion has been extracted from the crystal structure of HIV-RT (1RTD; HIV polymerase + template + primer + Mg^{2+} + natural substrate)[18] to incorporate into our model structure of HCV RdRp complex. A similar right hand structure (Fig. 2a: fingers, palm, and thumb subdomains)[36] were assigned for the modeled structure with respect to HIV RT. The model structure was optimized and prepared using Protein Preparation Wizard (PPW) module of Maestro interface. The obtained structure was submitted for a short minimization through Impref module of PPW followed by a MacroModel[37] minimization employing OPLS2005 force field with 5000 iterations. A dynamic simulation of 5 ns was performed through Desmond[38] in explicit solvent system to observe the stability of HCV RdRp complex system. The average structure was minimized through MacroModel to generate the final model structure (Fig. 2a). The 3D structures of all preliminary designed molecules (Type **IV**) and their triphosphate forms were built using Maestro and treated in LigPrep to optimized ligand conformer. The conformational search was conducted through MacroModel using MMFFs force field to obtain the most favored conformations. The lowest energy conformer was selected to perform molecular docking studies. Receptor grid was generated around ATP (the natural nucleoside triphosphate) using Glide receptor grid generation utility. The docking of triphosphate form of ligands at the predefined receptor grid were conducted using XP (extra precision) mode of Glide[20] to investigate the binding mode and binding score. The docked poses were rescored using Prime[35] with MMGBSA free energy of binding, which includes ligand-HCV RdRp interaction energy (DG: Table 1). The MMGBSA scoring is based on the difference between the energy of the ligand bound complex and sum of the energy of unbound HCV RdRp [$E_{binding} = E_{complex} - (E_{protein} + E_{ligand})$]. The lowest energy conformer of all selected molecules (Table 1) was submitted for drug like properties analysis using QikProp module of Schrodinger.

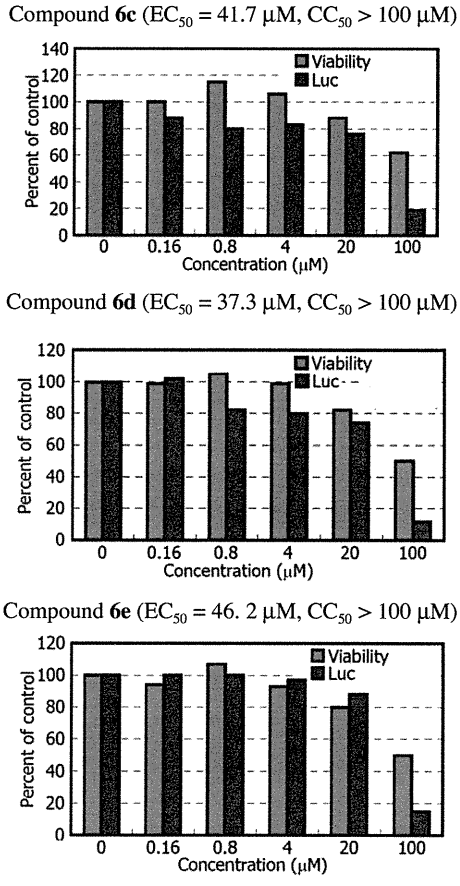

Figure 5. Anti-HCV activity of **6c–e** in replicon cells.

All compounds were dissolved in dimethyl sulfoxide (DMSO) at a concentration of 20 mM or higher to exclude the cytotoxicity of DMSO and stored at −20 °C until use. Huh-7 cells containing self-replicating subgenomic replicons with a luciferase reporter, LucNeo#2,[39] were grown and cultured in Dulbecco's modified Eagle medium with high glucose (Gibco/BRL) supplemented with 10% heat-inactivated fetal bovine serum (Gibco/BRL), 100 U/ml penicillin G, and 100 μg/ml streptomycin. LucNeo#2, were maintained in culture medium containing 1 mg/ml G418 (Nakarai Tesque). The anti-HCV activity of the test compounds was determined in LucNeo#2 cells by the previously described method with some modifications.[40] Briefly, the cells (5×10^3 cells/well) were cultured in a 96-well plate in the absence of G418 and in the presence of various concentrations of the compounds. After incubation at 37 °C for 3 days, the culture medium was removed, and the cells were washed twice with phosphate-buffered saline (PBS). Lysis buffer was added to each well, and the lysate was transferred to the corresponding well of a non-transparent 96-well plate. The luciferase activity was measured by addition of the luciferase reagent in a luciferase assay system kit (Promega) using a luminometer with automatic injectors (Berthold Technologies). The number of viable cells was determined by a dye method using the water soluble tetrazolium Tetracolor One® (Seikagaku Corporation), according to the manufacturer's instructions.

We have applied ligand-based bioisosteric replacement approach to design a new series of carbocyclic nucleoside where amino group at C-4 position (well known for H-bonding with RNA template) was replaced with a methyl group. The rational behind this approach was that the methyl group should be able to restore H-bonding through weak C–H...O interaction, which was observed in modeling studies. Although, this approach didn't yield any

highly active molecules, however, **6c–e** was found to be moderately active against HCV. The major advantages of these compounds are; limited cytotoxicity (CC_{50} > 100 μM) and better lipophilicity. Further synthetic exploration and biological evaluation are warranted to optimize this novel lead into potential anti-HCV nucleoside inhibitor.

Acknowledgments

This research received funding from DST, New Delhi, India through grant no SR/FT/CS-069/2009. A.T. and T.B. are thankful to DST, India for JRF. AS thanks DBT, New Delhi, India for modelling software support. A.S. & C.B. would like to dedicate this manuscript to Professor C. K. Chu. Authors acknowledge ILS, Hyderabad for NMR-Mass Facility and CIF, BIT Mesra for analytical support.

Supplementary data

Supplementary data associated with this article can be found, in the online version, at http://dx.doi.org/10.1016/j.bmcl.2012.09.072.

References and notes

1. Lavanchy, D. *Clin. Microbiol. Infect.* **2011**, *17*, 107.
2. Di Bisceglie, A. M.; McHutchison, J.; Rice, C. M. *Hepatology* **2002**, *35*, 224.
3. Lavanchy, D. *Liver Int.* **2009**, *29*, 74.
4. Ishii, K.; Tanaka, Y.; Yap, C. C.; Aizaki, H.; Matsuura, Y.; Miyamura, T. *Hepatology* **1999**, *29*, 1227.
5. McCown, M. F.; Rajyaguru, S.; Le Pogam, S.; Ali, S.; Jiang, W. R.; Kang, H.; Symons, J.; Cammack, N.; Najera, I. *Antimicrob. Agents Chemother.* **2008**, *52*, 1604.
6. Carroll, S.; Olsen, D. *Infect. Disord. Drug Targets* **2006**, *6*, 17.
7. Eldrup, A. B.; Allerson, C. R.; Bennett, C. F.; Bera, S.; Bhat, B.; Bhat, N.; Bosserman, M. R.; Brooks, J.; Burlein, C.; Carroll, S. S. *J. Med. Chem.* **2004**, *47*, 2283.
8. Eldrup, A. B.; Prhavc, M.; Brooks, J.; Bhat, B.; Prakash, T. P.; Song, Q.; Bera, S.; Bhat, N.; Dande, P.; Cook, P. D. *J. Med. Chem.* **2004**, *47*, 5284.
9. Cho, A.; Saunders, O. L.; Butler, T.; Zhang, L.; Xu, J.; Vela, J. E.; Feng, J. Y.; Ray, A. S.; Kim, C. U. *Bioorg. Med. Chem. Lett.* **2012**, *22*, 2705.
10. Kim, H. J.; Sharon, A.; Bal, C.; Wang, J.; Allu, M.; Huang, Z.; Murray, M. G.; Bassit, L.; Schinazi, R. F.; Korba, B.; Chu, C. K. *J. Med. Chem.* **2009**, *52*, 206.
11. Zhang, H. W.; Zhou, L.; Coats, S. J.; McBrayer, T. R.; Tharnish, P. M.; Bondada, L.; Detorio, M.; Amichai, S. A.; Johns, M. D.; Whitaker, T.; Schinazi, R. F. *Bioorg. Med. Chem. Lett.* **2011**, *21*, 6788.
12. Crimmins, M. T. *Tetrahedron* **1998**, *54*, 9229.
13. Zhu, X. F. *Nucleosides Nucleotides Nucleic Acids* **2000**, *19*, 651.
14. Ferrero, M.; Gotor, V. *Chem. Rev.* **2000**, *100*, 4319.
15. Schneller, S. W. *Curr. Top. Med. Chem.* **2002**, *2*, 1087.
16. Wang, J.; Rawal, R. K.; Chu, C. K. *Med. Chem. Nucleic Acids* **2011**, *16*, 1.
17. Balaraju, T.; Bal, C.; Sharon, A. *Antiviral Res.* **2012**, A14.
18. Huang, H.; Chopra, R.; Verdine, G. L.; Harrison, S. C. *Science* **1998**, *282*, 1669.
19. Mosley, R. T.; Edwards, T. E.; Murakami, E.; Lam, A. M.; Grice, R. L.; Du, J.; Sofia, M. J.; Furman, P. A.; Otto, M. J. *J. Virol.* **2012**, *86*, 6503.
20. Glide-V-5.7. Schrödinger, LLC., New York, NY, **2011**.
21. Schrödinger. LLC, New York, NY, **2011**.
22. Lipinski, C. A.; Lombardo, F.; Dominy, B. W.; Feeney, P. J. *Adv. Drug Delivery Rev.* **2001**, *46*, 3.
23. Duffy, E. M.; Jorgensen, W. L. *J. Am. Chem. Soc.* **2000**, *122*, 2878.
24. Jorgensen, W. L.; Duffy, E. M. *Adv. Drug Delivery Rev.* **2002**, *54*, 355.
25. Cho, J. H.; Bernard, D. L.; Sidwell, R. W.; Kern, E. R.; Chu, C. K. *J. Med. Chem.* **2006**, *49*, 1140.
26. Ohira, S.; Sawamoto, T.; Yamato, M. *Tetrahedron Lett.* **1995**, *36*, 1537. $[\alpha]_D^{23}$ + 28.4 (*c*, 1.00, $CHCl_3$); Compound **1** $[\alpha]_D^{29}$ + 30.9 (*c*, 1.00, $CHCl_3$).
27. Hocek, M.; Pohl, R.; Císařová, I. *Eur. J. Org. Chem.* **2005**, *2005*, 3026.
28. General method for the preparation of **6a–e**.
To a mixture of appropriate **3a–e** (1.5 mmol), **1** (1.57 mmol) and Ph_3P (3.75 mmol) in THF was added DIAD (3.75 mmol) dropwise at 0 °C under nitrogen and stirring continued at rt. Completion of reaction was analyzed by TLC, solvent evaporated under reduced pressure and crude was purified by column chromatography on silica gel by eluting up to 30 % ethyl acetate in hexane to give couple products in more than 80 % yield. The deprotection was carried out by heating at 60 °C in 10 % HCl in MeOH. After completion (monitored by TLC), the reaction mixture was neutralized by $NaHCO_3$ and purified by silica gel chromatography (10% methanol in DCM) to get **6a–e** in 70–85% yield.
Data for (1*S*,2*R*,5*R*)-3-(hydroxymethyl)-5-(4-methyl-7*H*-pyrrolo[2,3-*d*]pyrimidin-7-yl)cyclopent-3-ene-1,2-diol (**6a**): Yield: 80 %; mp: 168–170 °C; MS-ESI (*m*/*z*): [M⁺+1] 261.9; $[\alpha]_D^{21}$: – 101.70 (*c* 0.24, MeOH); UV (MeOH) λ_{max} 269 nm; ^{1}H NMR (400 MHz, DMSO-d_6): δ 2.64 (s, 3H), 4.12–4.17 (m, 3H), 4.44 (t, *J* = 5.6 Hz, 1H), 4.88–4.94 (m, 2H), 5.02 (d, *J* = 7.2 Hz, 1H), 5.63–5.67 (m, 2H), 6.70 (d, *J* = 3.6 Hz, 1H), 7.43 (d, *J* = 4 Hz, 1H), 8.64 (s, 1H); ^{13}C NMR (100 MHz, DMSO-d_6): δ 21.01, 58.55, 63.90, 72.31, 77.17, 99.25, 117.59, 123.98, 126.22, 149.90, 150.16, 150.54, 158.57.
Data for (1*S*,2*R*,5*R*)-5-(5-bromo-4-methyl-7*H*-pyrrolo[2,3-*d*]pyrimidin-7-yl)-3-(hydroxymethyl)cyclopent-3-ene-1,2-diol (**6d**): Yield: 81 %; mp: 215–217 °C; MS-ESI (*m*/*z*): [M⁺] 339.8 [M⁺+2] 341.8; $[\alpha]_D^{22}$ – 130.39 (*c* 0.21 MeOH-H_2O); UV (MeOH) λ_{max} 269.8 nm, 301.7 nm; ^{1}H NMR (400 MHz, DMSO-d_6) δ 2.84 (s, 3H), 4.12–4.17 (m, 3H), 4.44 (t, *J* = 5.6 Hz, 1H), 4.88 (t, *J* = 5.6 Hz, 1H), 4.95 (d, *J* = 6 Hz, 1H), 5.06 (d, *J* = 7.2 Hz, 1H), 5.63 (d, *J* = 1.2 Hz, 1H), 5.68 (bs, 1H), 7.68 (s, 1H), 8.68 (s, 1H); ^{13}C NMR (100 MHz, DMSO-d_6) δ 21.33, 59.04, 64.71, 72.74, 77.44, 87.18, 115.77, 123.93, 126.89, 149.61, 151.22, 151.60, 159.43.
29. Method for synthesis of (**6f**).
A suspension of **6e** (0.25 mmol), $Pd(PPh_3)_4$ (0.02 mmol), CuI (0.05 mmol) and Et_3N (0.77 mmol) in anhydrous DMF was purged with nitrogen at rt. Tributylvinyltin (2.58 mmol) was added under nitrogen and the mixture was stirred at 50 °C. The completion of reaction was checked by TLC, solvent was removed and residue was purified by on silica gel (100–200 mesh) column chromatography by eluting with 10 % methanol in DCM.
Data for (1S,2R,5R)-3-(hydroxymethyl)-5-(4-methyl-5-vinyl-7*H*-pyrrolo[2,3-*d*]pyrimidin-7-yl)cyclopent-3-ene-1,2-diol (**6f**): Yield: 72 %; mp: 148–150 °C; MS-ESI (*m*/*z*): [M⁺+1] 287.9; $[\alpha]_D^{22}$ – 157.66 (*c* 0.11 MeOH-H_2O); UV (MeOH) λ_{max} 269.5 nm, 310.7 nm; 1H NMR (400 MHz, DMSO-d_6) δ 2.75 (s, 3H), 4.13–4.22 (m, 3H), 4.44 (t, *J* = 5.2 Hz, 1H), 4.92 (t, *J* = 5.6 Hz, 1H), 4.96 (d, *J* = 6.4 Hz, 1H), 5.06 (d, *J* = 7.2 Hz, 1H), 5.19 (d, *J* = 11.2 Hz, 1H) , 5.63 (bs, 1H), 5.63–5.68 (m, 1H), 5.63–5.68 (bs, 1H), 7.01–7.08 (m, 1H), 7.70 (s, 1H), 8.62 (s, 1H); ^{13}C NMR (100 MHz, DMSO-d_6) δ 22.85, 58.56, 63.77, 72.27, 77.13, 113.56, 113.81, 115.24, 122.86, 123.88, 128.46, 150.16, 150.22, 150.52, 158.89.
30. Method for synthesis of (1*S*,2*R*,5*R*)-5-(5-ethynyl-4-methyl-7*H*-pyrrolo[2,3-*d*]pyrimidin-7-yl)-3-(hydroxymethyl)cyclopent-3-ene-1,2-diol (**6g**)
A suspension of **6e** (0.25 mmol), $Pd(PPh_3)_4$ (0.02 mmol), CuI (0.05 mmol) and Et_3N (0.77 mmol) in anhydrous DMF was purged with nitrogen at rt. Trimethylsilylacetylene (2.58 mmol) of was added under nitrogen and the mixture was stirred at rt. The completion was checked by TLC, solvent was removed and residue was purified on silica gel (100–200 mesh) chromatography by eluting with 10 % methanol in DCM to give trimethylsilyl protected compound in 80 % yield. The deprotection was done by stirring in methanol and K_2CO_3 (0.1 mmol) at rt for 2 h and purified by silica gel chromatography by eluting up to 10 % methanol in DCM to get **6g** as a light brown solid in 75 % yield.
31. Salim, M. T.; Aoyama, H.; Sugita, K.; Watashi, K.; Wakita, T.; Hamasaki, T.; Okamoto, M.; Urata, Y.; Hashimoto, Y.; Baba, M. *Biochem. Biophys. Res. Commun.* **2011**, *415*, 714.
32. Bressanelli, S.; Tomei, L.; Roussel, A.; Incitti, I.; Vitale, R. L.; Mathieu, M.; De Francesco, R.; Rey, F. A. *PNAS* **1999**, *96*, 13034.
33. Bressanelli, S.; Tomei, L.; Rey, F. A.; De Francesco, R. *J. Virol.* **2002**, *76*, 3482.
34. Steitz, T. A.; Smerdon, S. J.; Jager, J.; Joyce, C. M. *Science* **1994**, *266*, 2022.
35. Prime-V-3.0, Schrödinger, LLC., New York, NY, **2011**.
36. Joyce, C. M.; Steitz, T. A. *J. Bacteriol.* **1995**, *177*, 6321.
37. MacroModel-V-9.9. Schrödinger, LLC., New York, NY, **2011**.
38. Desmond-V-3.0. Schrödinger, LLC., New York, NY, **2011**.
39. Goto, K.; Watashi, K.; Murata, T.; Hishiki, T.; Hijikata, M.; Shimotohno, K. *Biochem. Biophys. Res. Commun.* **2006**, *343*, 879.
40. Windisch, M. P.; Frese, M.; Kaul, A.; Trippler, M.; Lohmann, V.; Bartenschlager, R. *J. Virol.* **2005**, *79*, 13778.